Connection of a power plant with a 150 kV Fault Current Limiting High Temperature Superconducting Cable

Short circuit current and transient recovery voltage analysis

ing. V.S. Mehairjan

18 August 2010

MSc Thesis Committee:

Dr. ir. M. Popov

Prof. ir. W.L. Kling

Prof. Dr. J.J. Smit

ir. A. Geschiere

Contact: vandanamehairjan@yahoo.com

Type: Master of Science thesis

Author: Vandana- Devi S. Mehairjan

Company: Liandon (member of Alliander)

Keywords: High Temperature Superconductor- Fault Current Limiter- Transient Recovery Voltage- Short-circuit Current- EMTP-ATPDraw™- High Voltage

Delft University of Technology

Faculty of Electrical Engineering, Mathematics and Computer Science

Electrical Power Systems

ॐ

सहनाववतु सहनौ भुनक्तु सह वीर्यं करवावहै ।

तेजस्विनावधीतमस्तु मा विद्विषावहै ॥

ॐ

शान्तिः शान्तिः शान्तिः ।

Om

Sahana Vavatu Sahanau Bhunaktu Sahaveeryam Karavavahai

Tejas Vinavati Tamastuma vidhwishavahai

Om

Shanti Shanti Shanti

Translation:

May He protect both of us. May He nourish both of us. May we both acquire the capacity (to study and understand the scriptures). May our study be brilliant. May we not argue with each other. Om peace, peace, peace.

Brief explanation:

At the beginning of a class, the teacher and students generally recite this peace invocation together. Both seek the Lord's blessings for study that is free of obstacles, such as poor memory, or the inability to concentrate or poor health. They also seek blessings for a conducive relationship, without which communication of any subject matter is difficult. Therefore, this prayer is important for both the teacher and the student.

Preface

Electrical Power Engineering (EPE) has always played a big role in my life, because my father has done the same Master of Science study in the United States of America. After finishing my Pre-University Education (V.W.O.) I decided to start my EPE study at the Anton de Kom University of Suriname (October 2000).
After two years (2002), the situations of my life had changed and I came to live in the Netherlands and continued my study at the InHolland Hogeschool in Alkmaar. After one-and-a half year of studying, EPE was shut down and it was not possible to become an Electrical Power Engineer. At that moment I decided to proceed and finish my studies at the HAN University of Professional Education (Hogeschool van Arnhem en Nijmegen). Even though the total travel time was about four hours and I got home late in the evening, my goal was more important than the sacrifices I had to make. During that year (September 2004) I was an intern at Liandon (former NUON Tecno) and Corus and experienced for the first time in my life to "work" and study. At Liandon I did two projects about protective earthing of a sub-station and harmonic distortion. For Corus, I used Vision (Phase toPhase software) to model and recalculate the settings of the protection relays. After finishing my courses and my intern-projects I did my final Bachelor of Engineering project at Liandon and developed Thermal Dynamic Model for Two Winding Transformers, based on the IEC60076. This model is used for predicting the top-oil and hot-spot temperature in transformers.

After gaining my degree I started working at Liandon and in September 2006 I began with my EPE Master of Science study at the Delft University of Technology.
During my entire studies I have been a Liandon employee, I even experienced the unbundling of the company NUON. The network company Alliander was formed, that consists of business units Liander and Liandon. Liander manages the gas and electricity networks in its service area. Liandon designs and realises complex energy infrastructures.

In order to finish my Master of Science study I have done my final project at Liandon. The project was conceived by ir. Alex Geschiere and was accepted by Prof.ir. Will Kling. During the whole project I was intensely supervised and coached by associate professor dr.ir. Marjan Popov from the group of Electrical Power Systems (EPS), which is a research unit of the department Electrical Sustainable Energy (ESE) of the Faculty of Electrical Engineering, Mathematics and Computer Science (EEMCS).

Acknowledgement

For my strength and abilities to succeed in life I thank God and my loving parents, Sam and Chandra.

As eldest child of my family I thank my brothers, Ashis and Ravish for their love and consideration.

I am thankful for the support and encouragement given by my daily supervisor dr.ir. Marjan Popov. His knowledge in network-modeling and Power System Analysis are excellent and without his effort, my research would have taken much more time.

A special word of thanks goes to prof.ir. Will Kling, ir. Alex Geschiere, drs. Carolyn Levisson (student counselor) and to all my lecturers and staff of ESE.

Throughout my whole studies I can thank many people who have played an important role in my life. They have encouraged me to go on with my studies, because some years where quite turbulent. I have been guided a lot by my managers ing. Henk Keur and ing. Piet Berendes and I thank both for their contributions.

Finally I thank all other special people in my live, through my heart, for their remarkable attention and stimulation to reach my goal.

After defending my thesis I will precede my encouraging job at Liandon and will contribute my knowledge to my employer and our society.

Aalsmeer, 2010
ing. Vandana-Devi Santusha Mehairjan

Abstract

The demand for electric power keeps on growing and electrical power networks are becoming more interconnected. This is a trend in many countries of the world that is caused by increased customer requirements and advanced technological improvements. In order to meet the ever-increasing energy demand, the integration of new power sources in the grid is necessary. This is a big challenge due to bottlenecks such as transport capacity, voltage fluctuations, fault levels and reactive power. The great challenge lies in the design of a network, with a smooth voltage profile and limited short circuit currents.

The smart-grid vision and the newest High Temperature Superconducting (HTS) cable technologies, can offer solutions for these issues. HTS cables will have a smart behavior, because they have an improved non-linear voltage-current characteristic. This innovative characteristic is caused by the non-linear resistance of the HTS cable. During normal operation the cable resistance is very low, resulting in low energy losses and smoother voltage profile. While the non-linear resistance increases very fast during short circuits, a significant reduction is caused in the fault currents.

This physical Fault Current Limiting (FCL) cable property is analyzed for the connection of a power plant with a 150 kV FCL HTS cable. An EMTP-ATP draw model is developed by using MODELS language based on the $R \sim I_t$ characteristics of FCL HTS cable. Short-circuit current analysis are carried out for this model, with and without the FCL HTS cable. When a fault occurs and the results are compared, the FCL HTS cable is capable of limiting the fault current.

For this model the generator terminal voltage and the Transient Recovery Voltage (TRV) have been analyzed. When a three-phase to ground fault occurs, the generator terminal voltage stays within the specified limits. The results of the TRV analysis are compared with the standard value that is allowed by the IEC.

Contents

Part one: "Introduction to the research project"

In this part an introduction will be given so that the reader can understand the problems that electrical utilities face, due to an increasing energy demand. Furthermore, the research subject will be introduced in this part and how this can provide solutions for the mentioned problems. The problem definition, the approach and finally the thesis layout are also part of this introduction.

1. Introduction

1.1 Energy trend

Nowadays in our modern society electric power is unthinkable and the demand for it is ever-increasing, leading to congestions on our electrical grids. Electric companies face challenges if they want to keep on providing their customers electricity continuously. To increase the increasing demand of electricity, more energy should be generated and transported to the customers while keeping in mind the environmental issues the world has to deal with, at present.

Increase of generation plants

One of the major causes of global warming is burning fossil fuels and bulk transportations of electrical energy, in order to provide more electricity. These necessities could still be provided by heading to a sustainable energy future and in this way reducing greenhouse emission gasses.

Many methods of sustainable power generation, such as large scale off- and on shore wind farms, hydro-power, photovoltaic and bio mass, can be applied in order to replace conventional power generation.

On customer level other technologies can be mentioned: small wind turbines, solar modules, micro turbines and fuel cells. Introducing these new technologies we are moving towards lower-carbon generation technologies and the demand of electrical power will increase in combination with load conglomerates. These solutions will lead to two main bottle-necks. Due to the increase in generation power the dynamic short-circuit withstand will increase. This dynamic short-circuit with-stand can exceed the maximum allowable value of protection and other high-voltage components in the power network.
Another difficulty is that it is not possible to plan the exact location of natural resources like sun; wind and water, so bulk transportations of electrical energy will take place.

Aging grid infrastructure and overhead lines

The powerful, sophisticated electrical grid built up during the last century has served us well, but it is reaching its limits and moreover it is becoming an aging infrastructure. The transport capacity of the existing power grid will have to increase and is also facing environmental issues like CO_2- emissions, EM-emissions and visual impact (overhead lines, despite their efficiency). This asks for an efficient underground infrastructure, but bulk transmission through conventional cables causes high reactive power consumption, voltage drops and heat emissions and is extremely costly.

Taking into account all these obstacles, problems and limitations and turning this into a challenge will stimulate real innovative solutions. This way the continuation of supplying reliable, secure and high quality energy will be preceded. The application of High Temperature Superconducting (HTS) cable technology can provide solutions to the previously mentioned obstacles, due to the capabilities of the cable material.

High Temperature Superconducting (HTS) cable technology provides a solution by utilizing less wire and transmitting five times more electricity than currently used conventional cables or transmission lines.

A comparison between conventional cable technology and HTS cable technology is depicted in Figure 1.

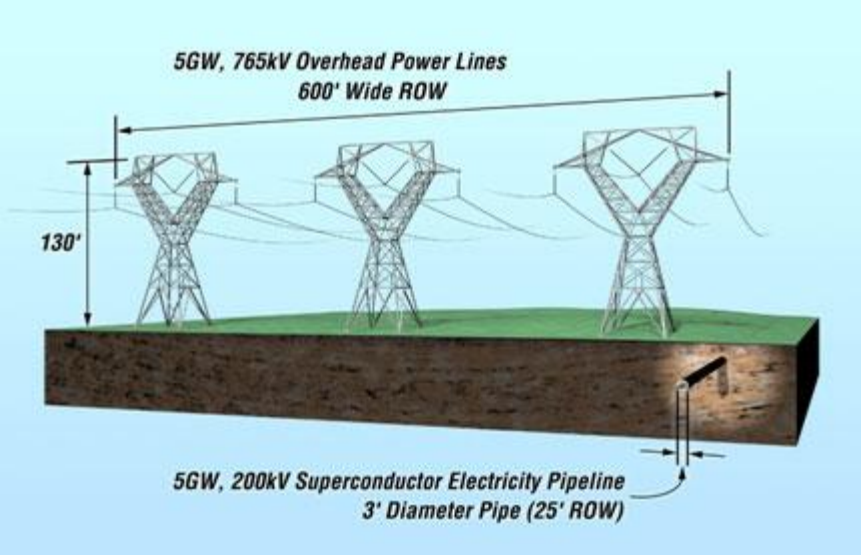

Figure 1: Comparison between overhead line and HTS cable
source: http://www.altenergymag.com/images/upload/Untitled-3.jpg

1.2 Research problem definition and objective

The increasing constraints in the location of generation plants, coupled with a strong emphasis on environmental sensibility, emerging trends in energy markets, and increasing reliability requirements, challenge the power industry to develop new technologies for the transmission and distribution systems. The key requirements that have to be fulfilled by these new technologies must be flexible, environmental friendly, efficient and reliable. High Temperature Superconducting (HTS) cable is one of the new technologies that can embody all of these important requirements. An example of a hypothetical smart grid, with HTS cable is depicted in Figure 2. In the future critical conventional network components will be replaced by superconducting counterparts, turning conventional electric components into smart grids.

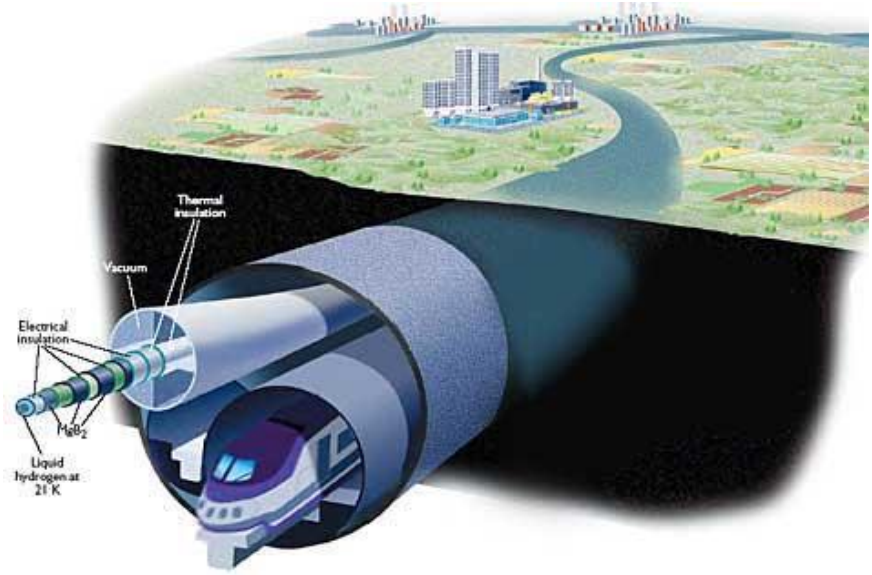

Figure 2: A hypothetical super grid energy pipe could share a tunnel with high-speed, long-distance trains.
source: (Paul Grant/Electric Power Research Institute/Ian Worpole)

Gradually HTS cable projects are being commissioned worldwide, the interest in this technology is increasing and pilot projects have succeeded. All these HTS cable projects have limited lengths of 200-600 m and are based on the “older” copper-core principle (that is energized during short-circuit currents. These types of cables are the so-called first generation superconducting cables; during normal operation the current flows through the superconducting material and when a fault occurs, the fault current will flow through a copper core.

The Dutch DSO Alliander, together with the NKT cables/Southwire joint venture Ultera, is currently conducting a study on the capabilities of a smart HTS cable for the (with a length of 6 km). The smart HTS cables have an improved non-linear voltage current characteristic that enables a smooth voltage profile during normal operation, while limiting the current during short-circuits and improving the grid’s stability.

The latest developments are to consider smart Fault Current Limiting (FCL) HTS cables in the transmission system (150 kV), when applying new generation sources to the grid. The integration of new generation sources in the transmission grid represents a big challenge due to bottleneck situations such as transport capacity, voltage fluctuations, fault levels and reactive power.

The short-circuit withstand capability of system components are often exceeded when a new power plant is connected with conventional cables to an existing grid, due to the increase of the short-circuit current. This means that it is difficult and challenging to apply new generators to the 150 kV transmission systems.

"In this research the aim is to prove that by making use of a smart FCL HTS 150 kV cable, instead of a conventional 150 kV cable, the short-circuit current flowing though the cable will decrease. With this in mind an analysis of the Transient Recovery Voltage will be carried out".

1.3 Approach

New generation plants need to be connected to the transmission power system, to fulfill the growth of the demand of electricity. In this research a conventional power system design will be used, for the implementation of FCL HTS cable technology to the 150 kV grid.

Traditionally, large-scale power sources like off-shore wind farms and conventional power plants, are not located near the customers. Through a high voltage transmission system, the power is transported to the regions where it is required.

In order to keep power losses as low as possible, many high-, extra-high and ultra-high voltages are created by large power transformers. To give an example, at a generator plant, the power is generated of approximately 20 kV voltage-level, through step-up transformers the voltage is stepped-up to for example 750 kV, 380 kV, or 150 kV. Transmission of power at high voltage level keeps power losses low, but creates other problems. Some of these difficulties are an increase in reactive power and insulation-coordination in high-voltage components. Furthermore, connecting new generation plant to an existing grid leads to an increase in short-circuit current contribution (in case of a fault).

Finally, when these complications are accepted and approached, the choice has to be made between underground-cables or visual overhead lines.

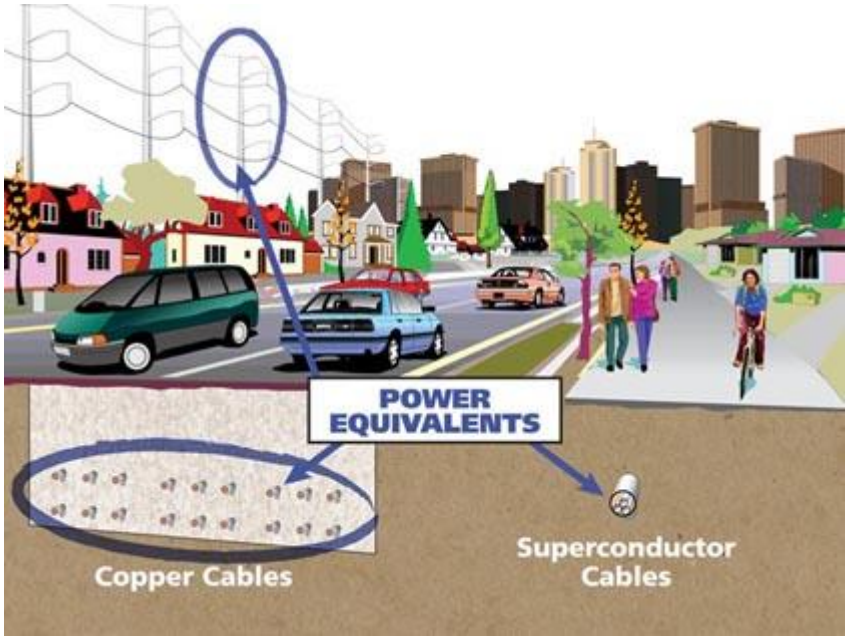

Figure 3: A smart infrastructure solution
source: http://www.amsc.com/images/Copper_vs_HTS_illo_0209_XS.jpg

Nowadays, overhead lines are not preferred, due to issues like visual impact and EM-emissions. Therefore, introducing an efficient underground infrastructure is necessary and this can be reached by applying HTS cable technology. In Figure 3 and Figure 4 two examples are depicted of how a future underground system should look like when HTS cable technology is applied instead of traditional methods.

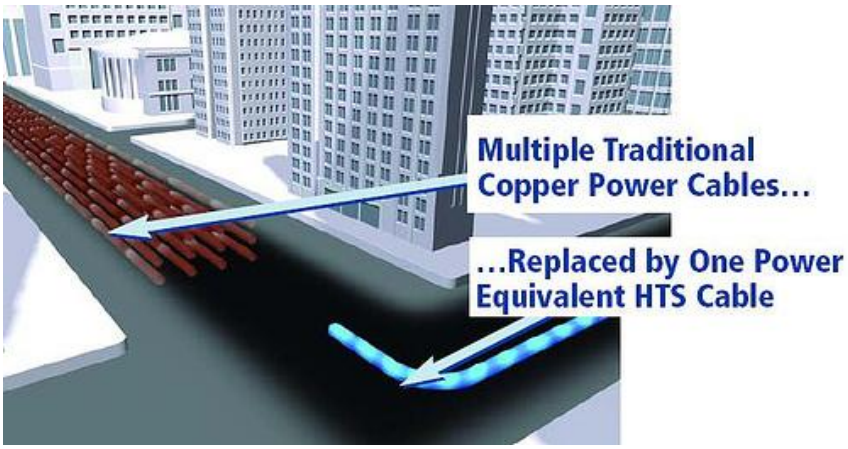

Figure 4: Future underground system
source:http://farm1.static.flickr.com/221/507891806_9019b5de19.jpg

Studied network

The interest has grown to analyze the application of a 150 kV HTS cable in the transmission network. Therefore, the 150 kV transmission network that is used for this research is represented in Figure 5.

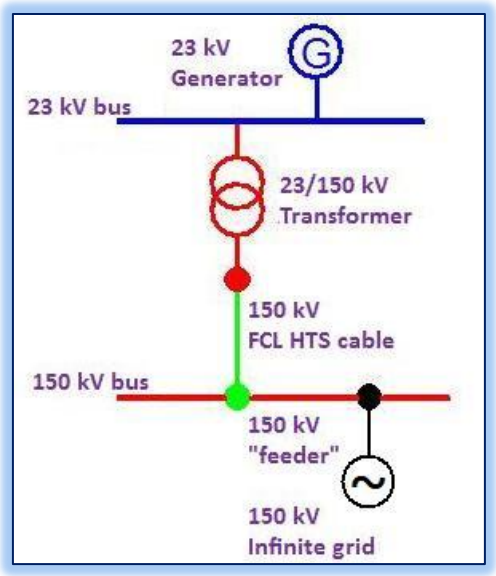

Figure 5: The studied 150 kV power system

The 150 kV bus is supplied by a 23 kV/550 MVA power plant, through a step-up transformer (23/150 kV). The 150 kV cable that supplies the 150 kV bus is a FCL HTS cable (= the studied cable). Three-phase faults will be simulated and analyzed for different locations in this electric circuit, with and without a FCL HTS cable. The Transient Recovery Voltage (TRV) that is caused by the limiting the fault

will also be simulated and the Rate of Rise of Recovery Voltage (RRRV) will be analyzed. The voltage across the generator terminals, at the moment of fault, is simulated.

1.4 Thesis layout

The thesis is split up in two parts and consists of several chapters. In the first part the reader is introduced to the research topic, the objective and the various aspects related to this topic. The network model, different component models, the software that is used for the analysis and the main reason for using a 150 kV FCL HTS cable, are also discussed in part one.

In the second part of the thesis, two important three-phase fault studies are defined and the following analyses/simulations are carried out:

- Short-circuit current analyses are carried out for both studied and the results of these fault studies are compared and analyzed with simulations without high temperature superconducting cable technology.
- The voltage across the generator terminals, at the moment of fault, is simulated.
- The results of Transient Recovery Voltage of the cable, for both fault studies, are analyzed.

In the end, conclusions and recommendations that arise from the results are presented.

2. High Temperature Superconducting (HTS) cables

In 1911 the discovery of the superconducting phenomenon was done by Kamerlingh Onnes, in Leiden, the Netherlands. He experimented with extreme low temperatures and made liquid helium for the first time. The scientist discovered that pure metal such as, mercury or lead become superconducting under very low temperatures. It took almost 75 years for material science to discover and develop new ceramic materials that have superconducting properties at relatively low temperatures. Ongoing research and development have led to the invention of superconducting materials in cable technology.

2.1 Physics of High Temperature Superconducting cables

HTS-cables use tapes made of superconducting material as current carrying elements. These elements can carry a current with practically zero losses as soon as their temperature falls below a temperature known as the "critical temperature" (T_c). The value of T_c depends on the type of superconducting material that is used for the HTS-tapes. Nevertheless, this physical phenomenon is influenced also by two other conditions: the current density and the magnetic field.
The superconducting state is achieved, when the temperature, current and magnetic field are below their critical values: T_c (critical temperature), I_c (critical current) and H_c(critical magnetic field). This behavior is schematically depicted in Figure 6 .

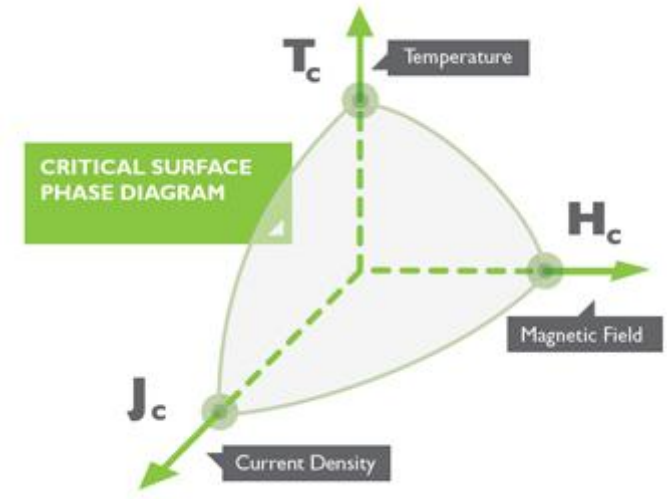

Figure 6: Critical surface diagram
(www.supercables.com)

2.2 Types of HTS cables

Two types of materials are used for HTS cables, BSCCO and YBCO. BSCCO is an alloy of Bismuth, Strontium, Calcium, Copper, and Oxide ($Bi_2SR_2CA_2Cu_3O_{10}$). These superconducting tapes have a multifilament structure and are called the first generation tapes.
The second generation superconducting material that is used for HTS tapes is a built of different layers. This multilayer tape has elements of Yttrium, Barium, Copper and Oxide ($YBa_2Cu_3O_7$). The functional difference is that the second generation tape has a higher critical current value, thus it is possible to transport more current through these types of cables. The costs for the second generation tapes are higher, but it is believed that the price will significantly become lower.

2.3 Principle designs HTS cables

Superconducting power transmission cables are available in two types (warm and cold dielectric type). The manufacturing process of the “warm dielectric” HTS cable is in principle not difficult, apart from the conductor. Its design is comparable to the design of conventional cables, whether it is the oil-filled or synthetic type. In the “warm dielectric” type the electric insulation (dielectric) is located outside the cryogenic cold part of the cable.
Even though the design of this type is relatively simple and has similarities to “older”/conventional cable technologies, there are quite a lot of disadvantages, for example higher electric losses, higher inductance, required phase separation to limit the effects of eddy current heating and control the production of stray electromagnetic fields (EMF) in the vicinity of the cable.
In the past several projects have been demonstrated using the technology of the “warm dielectric” HTS type, but due to the drawbacks there is no development in this area.

HTS cables available today are commonly referred to as “cold dielectric” HTS cables. The main reason for this description is due to the fact that the dielectric, or electrical insulation, of the cable is located inside the cable structure. Both types of cables are depicted in Figure 7.

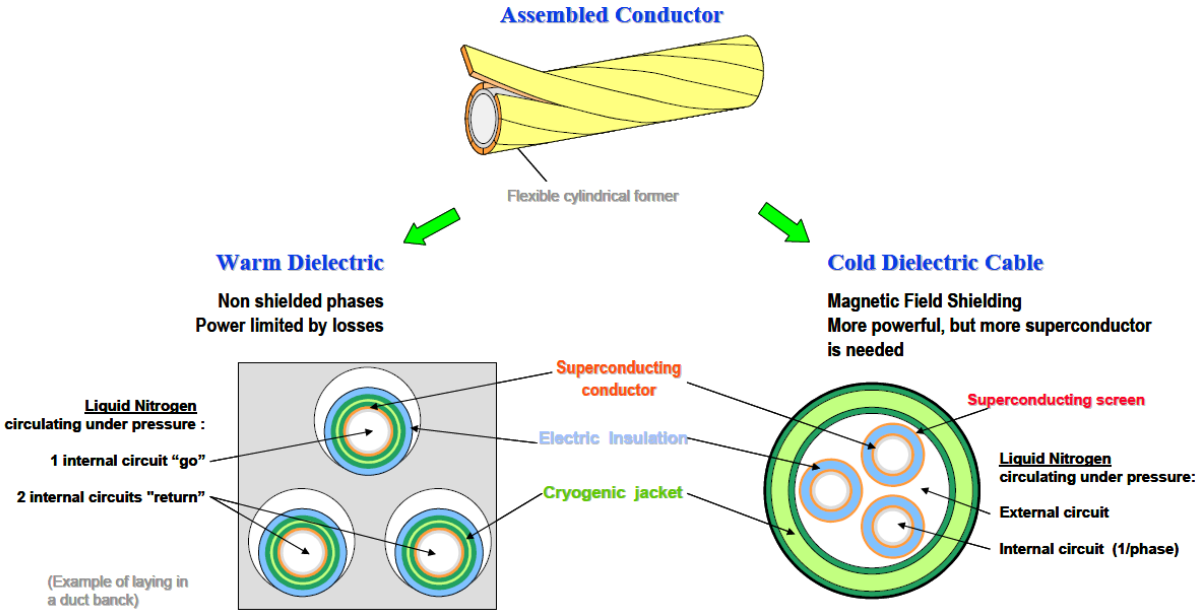

Figure 7: simplified design of Warm Dielectric and Cold Dielectric cable
source: Cigre study committee SC 21

In principle the manufacturing of the “warm dielectric” type is less complicated than the “cold dielectric” type, because the design is very close to that of conventional cables. The complicated and expensive manufacturing of the “cold cables” is caused by the structure of two superconductive components (internal and external circuit). Since the design is not common, it practically doubles the cost of the cable in comparison with the “warm dielectric” design. But this pays itself back in the advantage of canceling out the magnetic field outside the cable and so reducing losses.

For the operation of HTS cables, cooling systems are required to circulate liquid nitrogen through the system. This is necessary to evacuate the different types of losses: i) losses by conduction of heat through the walls of the cryogenic jacket, ii) electromagnetic losses in the superconductive materials; iii) losses due to viscosity of the circulating cooling fluid; iv) for the cold dielectric option, dielectric losses (1). The coolant medium is liquid nitrogen (LN).
The way of cooling and the cooling system will not be discussed in this thesis, because it is not in the scope of the research.

2.4 High Temperature Superconducting cable projects

In the past years many HTS cable projects in different parts of the world have been developed, constructed, demonstrated or completed. Most of the spectacular projects are briefly mentioned in this thesis, including the upcoming longest HTS cable project in the Netherlands.

In **Carlton, GA** (2000) a pioneering cable project was constructed and installed above ground level with three **31 m**, single-phase, HTS cables rated 12.4 kV, 1.25 kA. The partnership between Southwire and DOE made this project possible; the installed cables delivered power to Southwire manufacturing plants. The system operated continuously for 7 years at 100% load for over 40.000 hours and afterwards the cable was inspected. There was little to no significant degradation in the conductivity of the wire.

The development of another cable project began in **Albany, NY** (2001) with a partnership between DOE, New York State Energy Research and Development Authority (NYSERDA) and Superpower Inc. Further this team included BOC from Germany, Sumitomo Electric Industries (Osaka Japan) and National Grid (Westborough, MA) to the research group.
This major group started with the first phase on the Albany project, which consisted of a 320 meter long section connected to another 30 meter section of HTS cable made with first generation HTS wires. Afterwards, in 2006 this cable was removed, investigated and phase two of the project was introduced (in 2007). This phase consisted again a HTS cable of 30 m, but this time second generation HTS wires (2G wires) were used. It was the first time the use of 2G HTS wires were successfully demonstrated and completed.

A **200 m** HTS cable project was developed (2002) in **Columbus, OH** and energized in the Bixby substation (2006). The operating voltage of the cables is 13.2 kV and carries up to 3 kA; serving residential and industrial customers. The Columbus team included ULTERA (a joint venture of NKT cables of Denmark and Southwire), Oak Ridge National Laboratory, Praxair and American Superconductor. The cable that was used is called the TRIAX HTS cable, which consists of three concentric superconducting phases made of BSCCO-2223 HTS tape that are separated by layers of Cryoflex™ cold-dielectric tapes, which provides the phase-to phase electrical insulation.

The accomplishments of this project were great, because the amount of HTS tapes is reduced which makes this cable construction significantly cheaper; manufacturing and installation of the cable is simplified due to the presence of a single conductor; cooling and operation costs are significantly lower since a smaller surface needs to be cooled.

In **Long Island** (2008) the **first** HTS transmission-voltage power cable system was installed in a commercial power grid. The team that worked on this project consisted of American Supercondutor (AMSC), Long Island Power Authority (LIPA), DOE, Nexans and Air Liquide. Three 138 kV individual HTS power cables were installed, operated at full capacity and transmitted up to 574 MW of electricity. Later on in phase II of the Long Island project an existing cable was replaced by a **600 m** long 2G HTS wire. It is expected that this project will be completed in 2010.
A team of ULTERA, DOE, Oak Ridge National Laboratory and Entergy Corporation of **New Orleans** will install a 13.8 kV HTS cable to connect two existing substation sites in greater New Orleans. The scope of this project is to solve the electrical load problem and eliminating congestion on the power grid caused by high demands for electricity. This will be one of the longest HTS cable (**1.12 km**) and is expected to be energized in 2011.

In **Copenhagen, Denmark** (May 2001) a 30 kV, 2.4 kA HTS cable was installed by NKT cables. This was one of the first super-conducting cables that was installed in an electric power network, with a length of **30 m**. The purpose of this project was to provide energy to households and businesses on the island of Amager and to prove that the cable can operate under load variations, short-circuit currents and thermal & mechanical variations. After two years this project had succeeded and completed.

In the far East, the application of superconducting technology is also being developed. The **Korea** Electric Power Corporation (KEPCO) has done research on a **100 m** HTS cable with 22.9 kV class (power distribution level in Korea); and 1.25 kA which is five times the standard capacity of 250 A. This cable was installed at the KEPCO test site. In 2006 the commission test succeeded all necessary tests (commissioning test; operating with nominal current and voltage for 40 days; several heat and load cycle tests) and no abnormal responses were observed so far.

In **Japan** a new cable project has started, supported by Ministery of Economy, Trade and Industry (METI) and New Energy and Industrial Technology Development Organization (NEDO). The goal is to operate a 66 kV, 200 MVA HTS cable in the real grid and to demonstrate its reliability and stability. The grid is provided by Tokyo Electric Power Company (TEPCO) and SEI will manufacture the 3-in-one HTS cable (with a length between **200 and 300 m**), terminations and joints. The planning is to construct and operate this cable in 2011 and the operation period is scheduled for one year.

In the **Netherlands**, the longest HTS cable project of **6 km** will be placed, by the Dutch DSO Alliander, together with ULTERA. This project is a big challenge in HTS technology, due to the fact that this HTS cable will be the longest HTS cable, in the world. The so called Triax cable (Figure 8) will be used in this project.

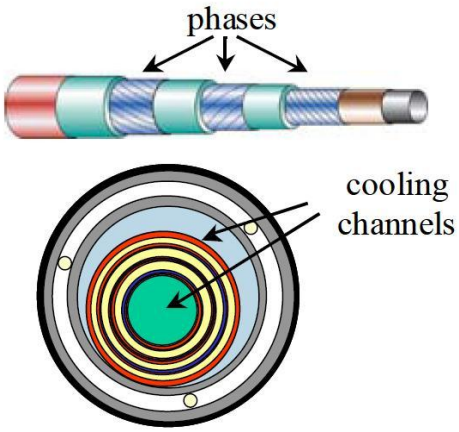

Figure 8: Triax cable

The Triax HTS cable is a smart cable, because it has an improved non-linear voltage-current characteristic that enables a smooth voltage during normal operation, while short-circuit currents are limited and the grid stability is improved.

Currently there is an ongoing research on the feasibility of the project, an efficient cooling system is designed and other technical issues are discussed. The planning is to demonstrate the potentials of the 6 km smart FCL HTS cable in 2015.

3. Methods for fault current limitation

The increase of power plants will cause a significant increase in fault current levels. At some points, the increase of the short-circuit current in the electric power system exceeds the maximum values. The generators, step-up transformers, circuit breakers and other components in the power system must be able to withstand the high short-circuit currents. In the following paragraphs different fault current limiting methods will be described.

3.1 System component impedance

The short-circuit current value can be *limited by the increasing impedance* of various system components, through which the fault current will flow. When designing a power system, these impedance values are taken into account, together with other interconnections of the system. In this way an initial approach is made to reduce the short-circuit current.

3.2 Fault current controllers and limiters

In many cases, the first approach of limiting the fault current is not enough. Another way of reducing the fault current is by *costly replacement of substation equipment* or by making changes in the configuration of the system. These changes can be done by *splitting the system* that may lead to decreased operational flexibility and lower reliability.

Moreover, fault current controllers can be applied, such as *simple inductors* or *variable resistors*. The disadvantage of applying these components is that in the normal state, energy is dissipated. Energy dissipation leads to unnecessary losses; unavoidable voltage drops and extra costs.

3.3 Fault Current Limiting High Temperature Superconducting cables

Fault Current Limiting High Temperature Superconducting (FCL HTS) cables have the property to limit the current during a short-circuit. In the superconducting state, which is during healthy operation of the grid, the FCL HTS cable is characterized by nearly zero resistance due to the low-loss nature of superconducting tapes that are used for these types of cables. In case of a fault, the FCL HTS cable will produce a certain value of a non-linear resistance and it is inserted into the power grid to limit the short-circuit current. A transition takes place from the superconducting to the normal state, the so-called quench.

In general, fast limitations of currents will lead to unacceptable high Transient Recovery Voltages (TRV). Due to the ***resistive*** limitation in FCL HTS cables the expectations are that the Rate of Rise of Recovery Voltage (RRRV) and the maximum level of the Transient Recovery Voltage (TRV) and the voltage on the generator terminals will stay within the limits. This is further considered in this thesis.

4. The Electromagnetic Transients Program (EMTP)

The Electromagnetic Transients Program (EMTP) is a computer program that can be used to solve electrical transient problems in lumped circuits, distributed circuits or combinations thereof. EMTP is used to model and analyze electrical systems in the time domain. And therefore, this program is used in this research for analyzing the application of the 150 kV FCL HTS in an electric circuit.

The Alternative Transient Program (ATP) is one of the versions of EMTP that is used world-wide in order to make digital simulations of transient phenomena of electromagnetic as well as electromechanical nature. ATPDraw™ for Windows is a graphical, mouse-driven preprocessor to the ATP version of the EMTP. In ATPDraw™ it is possible to create, edit and simulate the models of single or three-phase electrical networks, interactively. The electrical network can be constructed by the pre-defined components (standard- and TACS components) or by using MODELS. ATPDraw™ supports about 70 standard components and 23 TACS objects.

With these features this digital program provides possibilities to simulate complex networks and control systems of every type. EMTP/ATP has many modeling possibilities and important features, apart of the computation of transients.
The ATP program calculates variables of interest within electric power networks as functions of time, typically initiated by some disturbances. Basically, the trapezoidal rule of integration is used to solve the differential equations of system components in the time domain. Non-zero initial conditions can be determined either automatically by a steady-state, phasor solution or they can be entered by the user for some components (2).

TACS (Transient Analysis of Control Systems) is used for time-domain analysis of control systems. MODELS in ATP is a general-purpose description language supported by an extensive set of simulation tools for the representation and study of time-variant systems. MODELS allows the description of arbitrary user-defined control and circuit components, providing a simple interface for connecting other programs/models to ATP. As a general-purpose programmable tool, MODELS can be used for processing simulation results either in the frequency domain or in the time domain (2).

5. Network model and assumptions

5.1 Dutch transmission network

The (*national*) power grid in the Netherlands (depicted Figure 9) consists of 380 kV-, 220 kV-, 150 kV- and 110 kV lines and interconnections to the (*foreign*) European grid. The distribution network (50 kV and lower) is not shown on the map but it covers the whole country and it is mainly built up of underground cables.

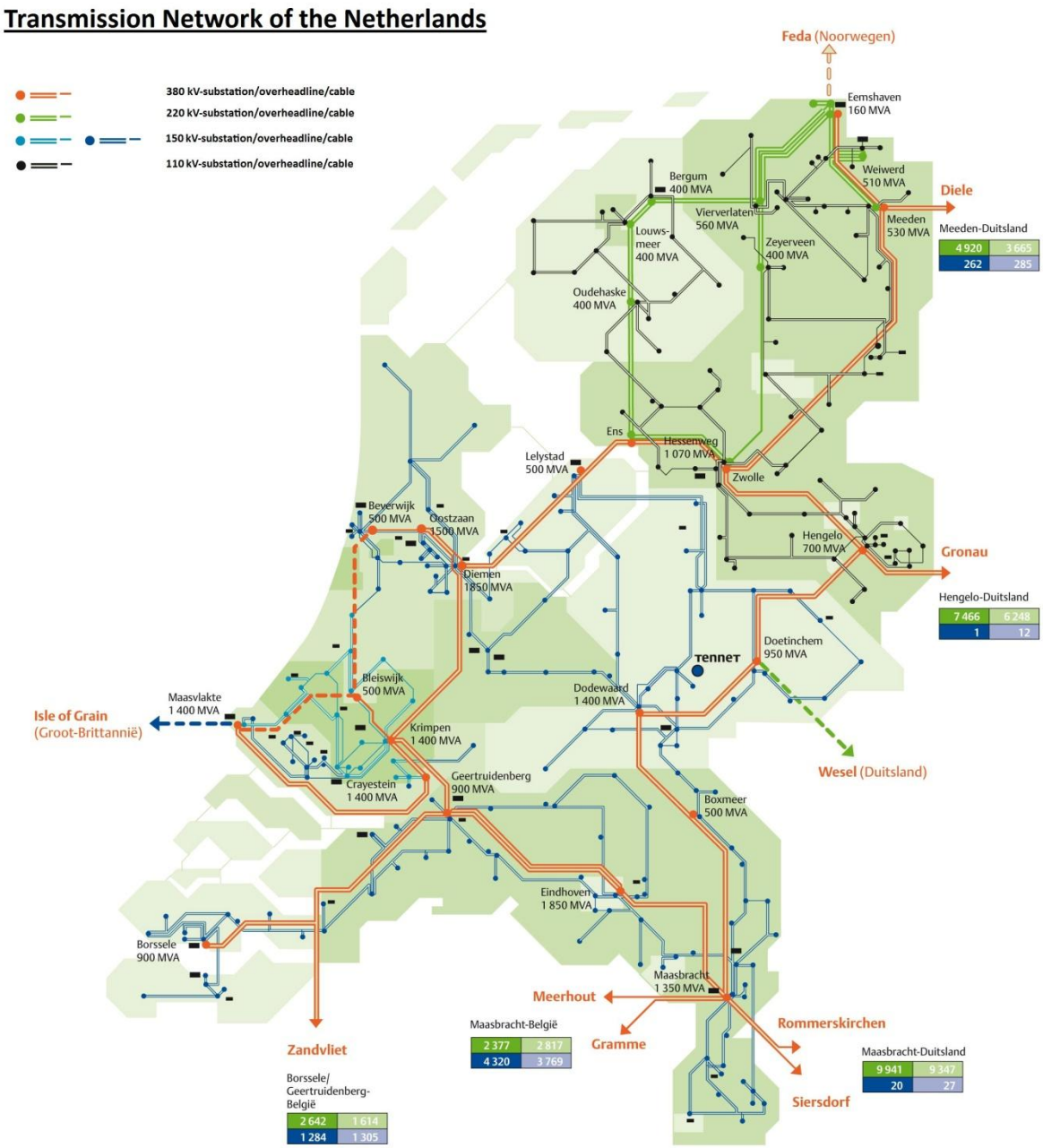

Figure 9: Dutch Transmission Network

5.2 Studied network model

The application of the HTS cables in the power network is interesting for voltage levels from 10 kV to 150 kV. Due to the high ampacity, higher voltage levels are not necessary [1]. This is the main reason for using a 150 kV FCL HTS cable and analyzing the 150 kV network. The 150 kV network will be represented as an infinite powerful grid in the simulation model and is connected to a new 23 kV power generator, as depicted in Figure 10. The generator is connected to a 23/150 kV step-up transformer. Through a 150 kV FCL HTS cable, the transformer is connected to the infinite 150 kV grid.

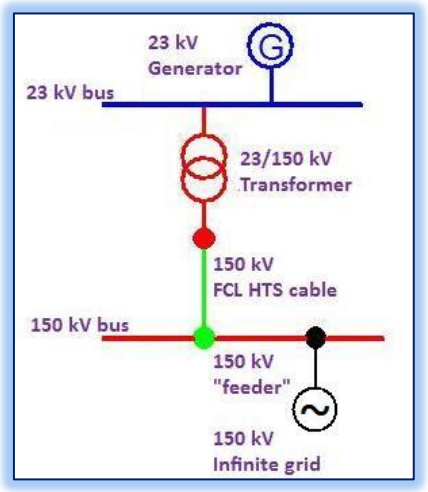

Figure 10: Schematic depiction of studied network

The system is studied for 50 Hz power frequency, with a wavelength of 6000 km. The wavelength of the sinusoidal currents and voltages is large compared with the physical dimensions of this network (cable length approximately 300 m). Logically, the network will be modeled by applying lumped elements and the travel time of the electromagnetic waves does not have to be considered. This makes it possible to model the network by using standard ATP components. To better understand the short-circuit simulations and TRV analysis, the studied system and ATP components will be explained (from left to right in Figure 11).

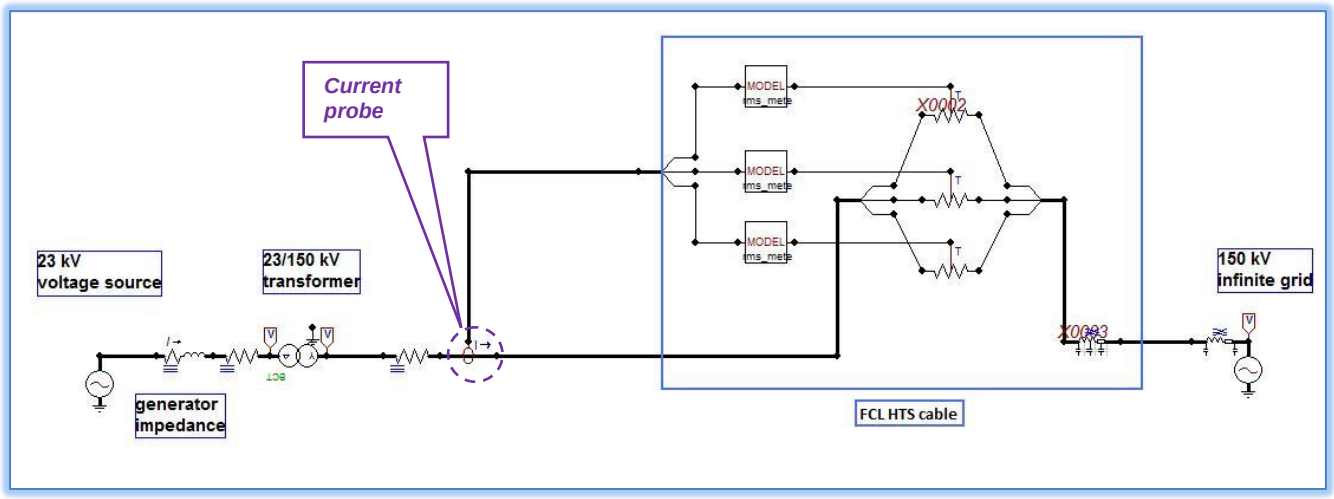

Figure 11: Studied network model in EMTP-ATPDraw

5.2.1 Generator Model

The generator is modeled as a voltage source and a RLC source impedance. Elements AC 3-ph type 14 (voltage source) and RLC 3-ph (impedance) are applied to represent the 23 kV generator and the generator impedance, where $Z_{generator} = \sqrt{(X"_d)^2 + R^2}$
R is the equivalent resistance and $X"_d$ is the sub-transient reactance of the generator. This reactance is used because $X"_d < X'_d < X_d$, which corresponds with $|I"| > |I'| > |I|$. This means that the reactances have increasing values and the corresponding components of the short-circuit current have decreasing magnitudes. For determining the interrupting capacity of circuit-breakers, the sub-transient reactance of the generator is used to obtain the initial current flowing on occurrence of a short-circuit.

The data input for the AC 3-ph type 14 voltage source and the RLC 3-ph impedance in this system are shown in the tables below. The maximum phase voltage amplitude is calculated by multiplying the phase to phase voltage with $(\frac{\sqrt{2}}{\sqrt{3}})$. The value for the resistance and inductance are calculated for a representative 23 kV generator in a 150 kV system.

DATA PARAMETER	UNIT	VALUE	SYMBOL
Max amplitude phase voltage	V	18779	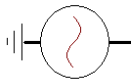
Frequency	Hz	50	
Phase shift	°	-90	

Table 1: AC 3-ph type 14 simulation data and symbol

DATA PARAMETER	UNIT	VALUE	SYMBOL
Resistance per phase	Ω	0,0265	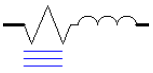
Inductance per phase	mH	0,858	

Table 2: RLC 3-ph simulation data and symbol

5.2.2 Transformer Model

The generator is connected to a 23/150 kV step-up transformer, which includes the short-circuit transformer impedance. The step-up transformer is a three-phase Δ/Y connected transformer and it delivers power to the 150 kV infinite grid (through the 150 kV FCL HTS cable). The magnetizing and saturation effects of the transformer are neglected. The BCTRAN supporting routine is used to model the transformer, which supports single-phase or three-phase (both shell and core type); 2-, 3- and multiple winding transformers; using the test data of both the exciting test and the short-circuit test at the rated frequency. Excitation and short-circuit losses can be taken into account by this transformer model. If zero sequence data is available, these can also be inserted in the model. Stray capacitances are ignored, for low frequencies up to a few kHz. The data parameters of the BCTRAN element are given in Table 3. The different values that are necessary for calculations are generated by ATP-draw by inserting factory test parameters (open- and short-circuit test). It must be noticed that only positive sequence parameters are available for the transformer used in this system.

DATA PARAMETER	UNIT	VALUE	SYMBOL
Number of phases		3	
Number of windings		2	
Test frequency	Hz	50	
Power	MVA	710	
Low Voltage	kV	23	
High Voltage	kV	150	
Connection	LV/HV	ΔY	
Phase shift	°	30	
FACTORY TEST DATA : OPEN CIRCUIT (POSITIVE SEQUENCE)			
DATA PARAMETER	**UNIT**	**VALUE**	
Voltage	%	100	
Current	%	0,156	
Loss	kW	300	
FACTORY TEST DATA : SHORT CIRCUIT (POSITIVE SEQUENCE)			
DATA PARAMETER	**UNIT**	**VALUE**	
Impedance	%	12,969	
Power	MVA	710	
Loss	kW	1100	

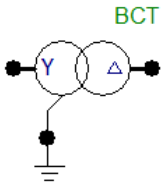

Table 3: BCTRAN simulation data and symbol

5.2.3 Cable model

Normally such an electrical network would be built by using overhead-transmission lines or conventional cables to connect the generator plant to the 150 kV grid. For this research a 150 kV FCL HTS cable will be used to couple the 150 kV infinite grid to the power plant, to simulate the fault current limiting effect of the cable. First of all the determination of the cable parameters is discussed, this is based on [1] and afterwards the implementation of these parameters in ATP is described.

5.2.3.1. Cable parameters and definition of non-linear resistance

The electric parameter model that is applied for the cable superconductor corresponds to an equivalent pi-model of a transmission line depicted in Figure 12 usually used in power system studies.

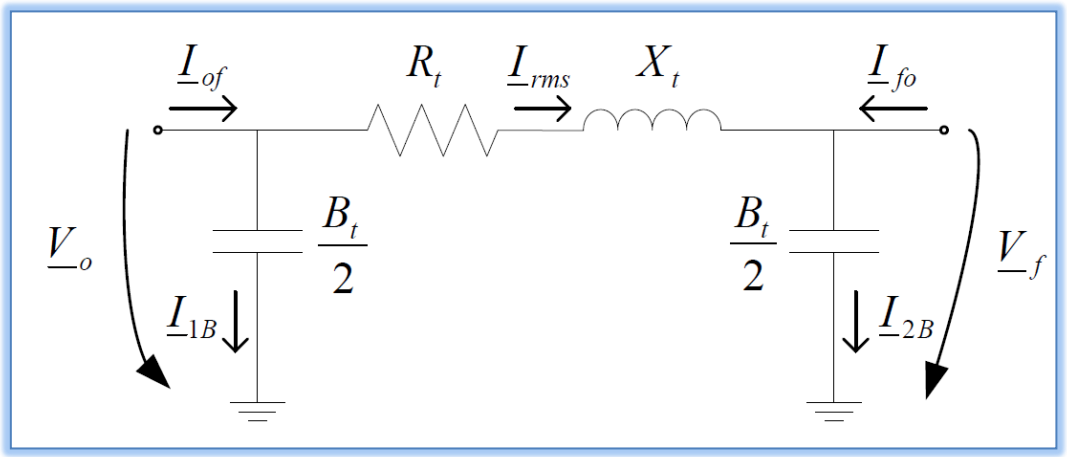

Figure 12: Equivalent pi-model of a transmission line [2]

In this pi-model: resistance R_t represents AC losses *)
reactance X_t represents magnetic field
susceptance B_t represents electric field

*) Due to the different behavior of the superconducting cables compared to conventional power lines, R_t will represent AC losses instead of joule effects.

X_t and B_t have the same physical origin in superconducting cables and in conventional transmission lines.

$$\boldsymbol{X_t = (\omega . L) . l} \quad [5.1]$$

$$\boldsymbol{B_t = (\omega . C) . l} \quad [5.2]$$

For this pi-model the capacitance and inductance per unit length are calculated.

$$L = \frac{\mu_0}{2\pi} \ln\left(\frac{r_s}{r_2}\right) \quad [5.3]$$

$$C = \frac{2\pi\varepsilon_0\varepsilon_r}{\ln\left(\frac{r_s}{r_2}\right)} \quad [5.4]$$

where ω is the base angular frequency,
l is the cable length,
μ_0 is the magnetic constant (= $4\pi.10^{-7}$),
r_s is the radius of the superconducting shield,
r_2 is the outer radius of one superconducting phase,
ε_0 is the electric constant and ε_r is the relative permittivity of the dielectric

The previous information is based on a publication [2], in this thesis the values of C and L are used from a conventional 150 kV cable. This is done under the assumption that these two parameters are nearly the same for superconducting cables, since they depend on the insulation of the cable.

The cable AC losses, P_{AC}, are expressed as a function of RMS-current, I_{rms}, for two states [2]:

$$P_{AC} = K_1 I_{rms}^{q1} \quad (I_{rms} < I_{nom}) \quad [5.5]$$

$$P_{AC} = K_2 I_{rms}^{q2} \quad (I_{rms} > I_{nom}) \quad [5.6]$$

where K_1, K_2, q_1 and q_2 are empirical parameters,
I_{rms} is RMS current trough the cable branch between original bus and end bus
I_{nom} is the superconducting cable nominal current

The conversion of the AC losses value to the resistance value is carried out, by using the following expression:

$$R_t = \frac{P_{AC}}{I_{rms}^2} \quad [5.7]$$

from [5.5] and [5.6] the following equations are defined for the resistance

$$R_t = K_1 I_{rms}^{q1-2} \quad (I_{rms} < I_{nom}) \quad [5.8]$$

$$R_t = K_2 I_{rms}^{q2-2} \quad (I_{rms} > I_{nom}) \qquad [5.9]$$

The following superconductor cable resistance parameters are obtained, by applying the previous equations and by using the information described in [2]:

$$R_t = 10^{-3,5555} I_{rms}^{0,1699} \quad (I_{rms} < I_{nom}) \qquad [5.10]$$

$$R_t = 10^{-18,041} I_{rms}^{4,9090} \quad (I_{rms} > I_{nom}) \qquad [5.11]$$

With this result and the R_t ~ I_{rms} characteristic given in equation [5.10] and [5.11], the following graph is plotted. Figure 13 defines R_t ~ I_{rms} characteristic that is used in MODELS of ATP for the superconductor cable.

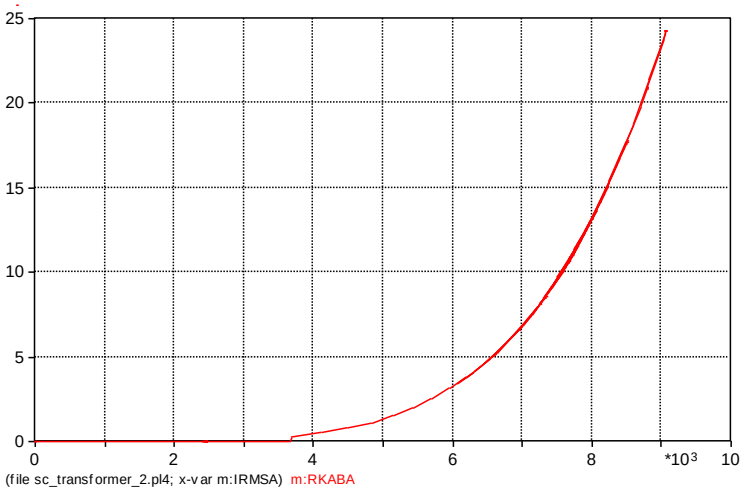

Figure 13: R_t ~ I_{rms} characteristic

In order to carry out dynamic short-circuit current analysis, based on the instantaneous current, the R_t ~ I_{rms} characteristic is rewritten. R becomes a function of time (I_t) and can generally be written as:

$$R_t = 10^x * I_t^a \qquad [5.12]$$

Critical current

In order to keep the AC losses low during normal operation, the critical current I_c, is chosen 30% higher than the nominal current, I_{nom}:

$$I_c = 1,3 * I_{nom} \qquad [5.13]$$

leading to:

$$R_t = 10^{-3,5555} |I_t|^{0,1699} \quad (I_t < I_c) \qquad [5.14]$$

$$R_t = 10^{-18,041} |I_t|^{4,9090} \quad (I_t > I_c) \qquad [5.15]$$

The first R_t ~ I_t characteristic is used when the cable is in the superconducting state (pre-fault condition).
When a fault occurs, a transition takes place from the superconducting state to the non-superconducting state, the so-called quench. If the value of the fault current is higher than the critical current, I_c, through the superconductor, the second R_t ~ I_t characteristic is used.

In the next steps the nominal current I_{nom} and critical current I_c for this superconductor cable are calculated. Both currents are based on the nominal current from the generator. In the following table the nominal current on the low-voltage (I_{nom_LV}) and high-voltage (I_{nom_HV}) side are calculated and eventually the value for the critical current is derived.

Generator: S = 520 MVA; U_{line} = 23 kV
$I_{nom\_LV} = \frac{S}{U_{line} * \sqrt{3}} = \frac{520.10^6}{23.10^3 * \sqrt{3}} = 13,05\ kA$
$I_{nom\_HV} = \frac{U_{LV}}{U_{HV}} * I_{nom\_LV} = \frac{23.10^3}{150.10^3} * 13,05\ kA = 2\ kA$
$I_c = 1,3 * (I_{nom\_HV} * \sqrt{2}) = 1,3 * (2kA * \sqrt{2}) = 3,67\ kA$

5.2.3.2. ATP cable model with non-linear resistance

In ATP the cable is modeled by using standard ATP-, TACS- and user specified components, by using MODELS. The fault current behavior of the superconducting cable is described as a non-linear resistance and standard cable capacitance and inductance. The non-linear resistance is constructed by using MODELS and TACS. In MODELS an algorithm is programmed to calculate the non-linear resistance of the cable, which is related to the momentarily current. The current through the circuit is measured and provided by a current-probe; this value is an input for the algorithm of MODELS; in MODELS the absolute momentarily current is calculated from the monitored current.
The absolute momentarily current is used for the determination of the non-linear resistance of the superconducting cable. This non-linear resistance is the output of MODELS and it is controlled by a TACS-controlled current-dependent resistance. Depending on the value of the momentarily current, the non-linear resistance will be low or will increase. The transition from the superconducting state

to the non-superconducting state, is programmed by making use of an “if-then-else” function in MODELS. Finally, the non-linear resistance model is connected to the rest of the cable components (inductance and capacitance), gaining the complete FCL HTS cable. The cable capacitance and inductance are modeled by using a standard π-circuit component, defined in ATP per unit length. This complete cable model is depicted in Figure 14 and all the cable components are named in this figure. Due to the resistive power dissipation in the cable, the energy is transferred into heat energy. The influence of the heat on the current limiting behavior of the cable is neglected in this research.

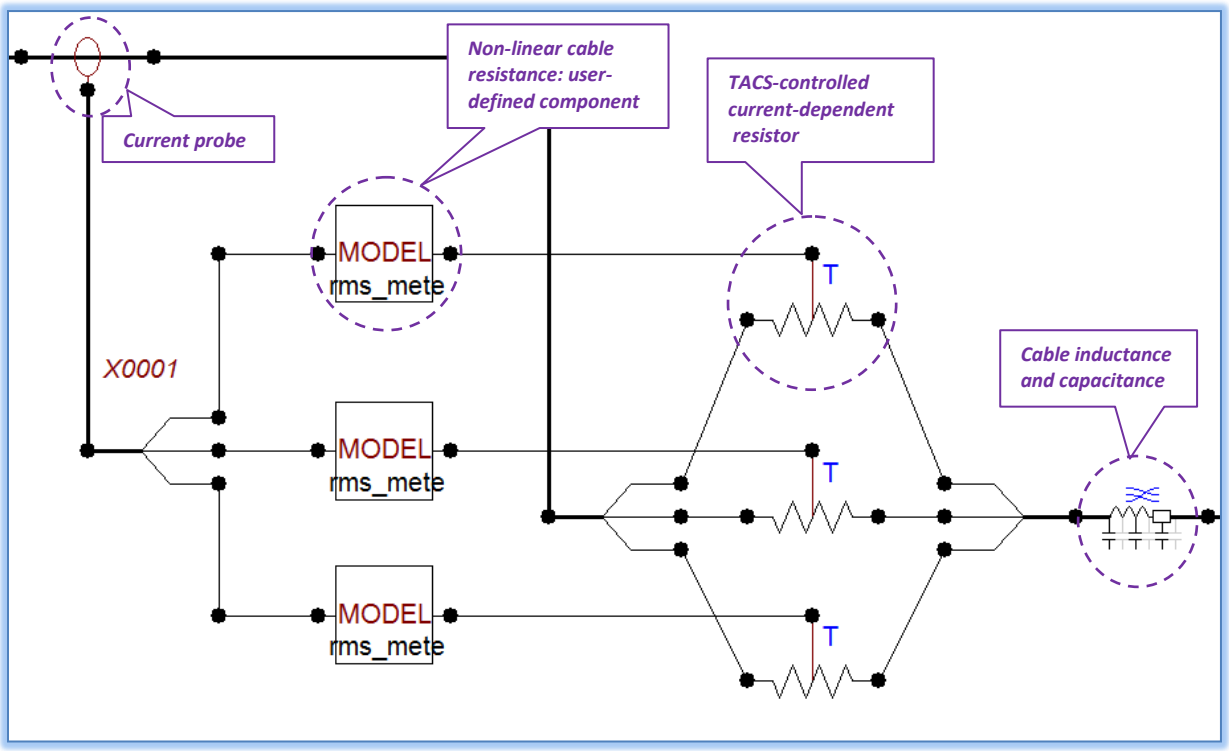

Figure 14: 150 kV FCL HTS Cable Model

5.2.4 Infinite grid model

The 150 kV infinite grid is modeled as a feeding voltage source (AC 3-ph type 14) and an impedance (RLC 3-ph). This is done in such a way that the short-circuit withstand current is above 40 kA_{rms} (specification of the grid). The data input for AC 3-ph type 14 and RLC 3-ph impedance in this system are shown in Table 4. The maximum phase voltage amplitude is calculated by multiplying the phase to phase voltage with $(\frac{\sqrt{2}}{\sqrt{3}})$.

DATA PARAMETER	UNIT	VALUE	SYMBOL
Max amplitude phase voltage	V	122254	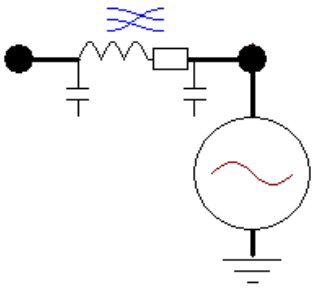
Frequency	Hz	50	
Phase shift	°	-90	
$R_{(positive)}$	Ω	0,2062	
$R_{(zero)}$	Ω	0,6	
$L_{(positive)}$	mH	6,56	
$L_{(zero)}$	mH	18	
$C_{(positive)}$	µF	1,0e-5	
$C_{(zero)}$	µF	1,0e-5	

Table 4: feeding source and impedance simulation data and symbol

In the rest of the network there are some very small resistances used (order 1 µΩ), to avoid numerical oscillations in calculations and keep the results stable.

5.2.5 Three-phase switch model

An ideal three-phase switch of the type SWIT_3XT is applied to simulate a three-phase fault to earth. During normal operation the switch is open and at a certain instant the switch will be closed. Depending on the fault location the fault current will be limited.
Both the three-phase fault current and the Rate of Rise of Recovery Voltage will be analyzed and modeled in different ways. For the fault current of the phases it is important to visualize the ***value of the peak current***; the total simulation time is 250 ms; the plotting time-step (Δt) is 2,5 μs; and on t = 100 ms a three-phase to earth fault is created. In Table 5 the simulation data and symbol of the three-phase switch is given.

DATA PARAMETER	UNIT	VALUE	SYMBOL
T-cl_phase_1	s	0,1	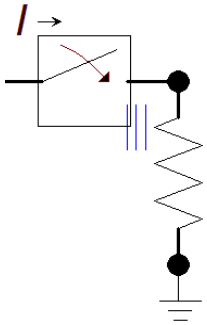
T-op_phase_1	s	1	
T-cl_phase_2	s	0,1	
T-op_phase_2	s	1	
T-cl_phase_3	s	0,1	
T-op_phase_3	s	1	
Output	A	current	
ATP SIMULATION SETTINGS: time domain			
DATA PARAMETER	**UNIT**	**VALUE**	
delta_T	s	$2{,}5.10^{-6}$	
Tmax	s	2,5	

Table 5: SWIT_3XT simulation data and symbol

For transients the ***steepness (du/dt) of the wave*** is important. Visualizing the waveform is not difficult, but analyzing the transient needs special settings in ATP due to the sensitivity of this result. The simulation time is very short (about 8 ms) and the time-step (Δt) is very small, 5 ns. This is done in order to get enough simulation time-steps and accurate results. In a following chapter the components used for the TRV-analysis will be discussed.

*All calculations are carried out with the assumption that the **superconductor is homogeneous** along its length. During normal operation the FCL HTS cable is in superconducting state.*

Part two: "Fault studies and results"

In this part the steady state conditions will be checked before the simulations are made. After that two fault study-simulations will be made and analyzed. These results will be discussed by comparing the same electrical power system, without a FCL HTS cable. The theory related to the main subjects of the analysis (short-circuit current and Transient Recovery Voltage analysis) will be mentioned during the case-study-discussions.

6. Steady-state operating conditions

The power system is in steady-state operating condition when all the measured (or calculated) physical quantities describing the operating condition of the system can be considered *constant* for purposes of analysis [3]. These criteria can be checked by simulating the voltage response of the ATP model of the studied scheme. The expectation is that the voltage response will be stable and the results will confirm that:

- the components are connected properly
- the input parameters of the components are correctly inserted
- the system has fulfilled the steady-state criteria

In order to investigate if the model with a FCL HTS cable fulfills the preceding expectations, the voltage on certain nodes will be verified. If there would be a load connected to the network, it would also be possible to monitor the power flow. The following node-voltages are simulated in order to verify the steady-state operating conditions:

1. The voltage response in steady state of the 23 kV generator is shown in Figure 15.
   From this graph it can be seen that the amplitude of the voltage is 18,8 kV, which is a data input parameter. Further it can be seen the generator emfs are equal in magnitude and displaced from each other 120 degrees in phase.

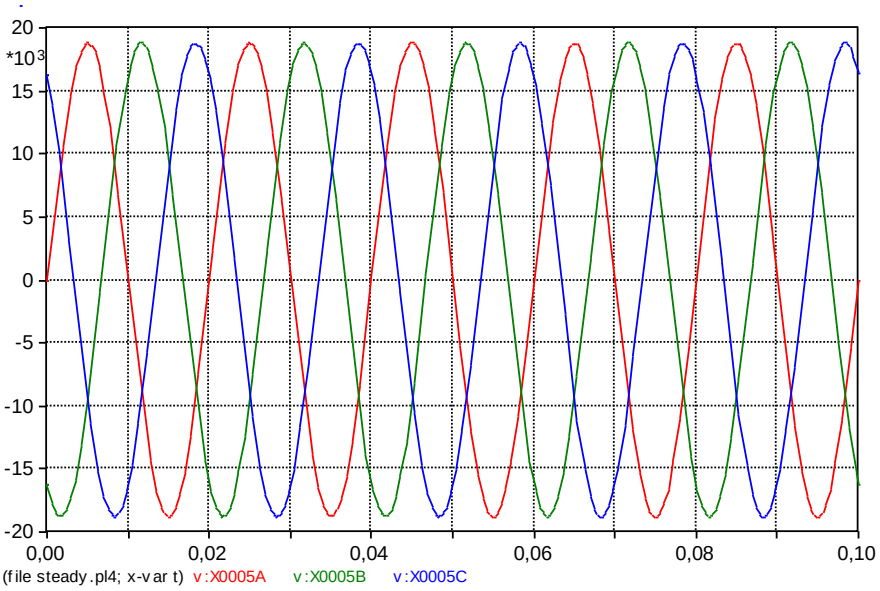

Figure 15: Voltage response of the generator (x-axis: time in s; y-axis: voltage in V)

2. The voltage in steady state at the low-voltage side (23 kV) and on the high-voltage side (150 kV) of the step-up transformer are depicted in the graphs of figure 17 and 18.

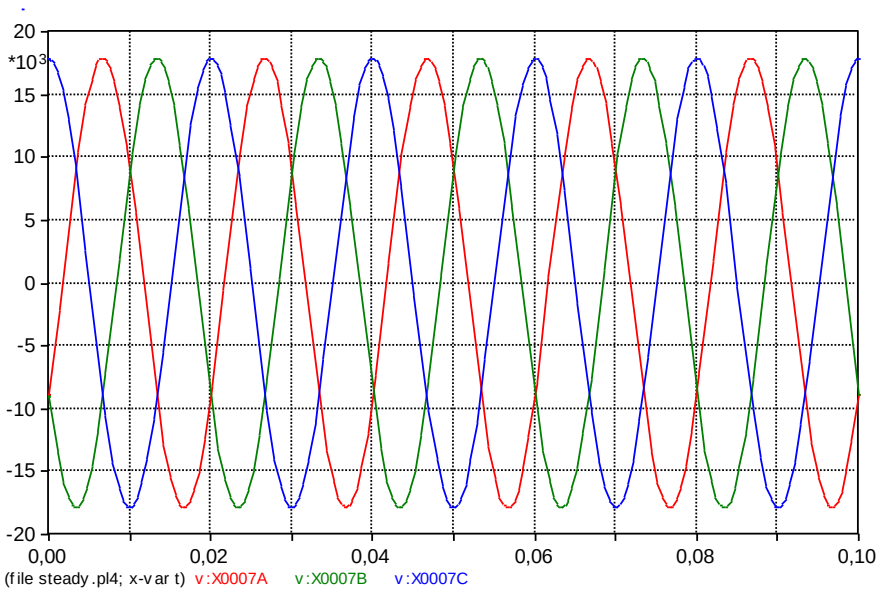

Figure 16: Voltage response on the low voltage side (23 kV) of the transformer (x-axis: time in s; y-axis: voltage in V)

In the following graph the voltage at the high-voltage side of the transformer is depicted. The peak value is in accordance with $V_{peak} = V_{rms} * \left(\frac{\sqrt{2}}{\sqrt{3}}\right) = 150\ kV * \left(\frac{\sqrt{2}}{\sqrt{3}}\right) = 122{,}5\ kV$.

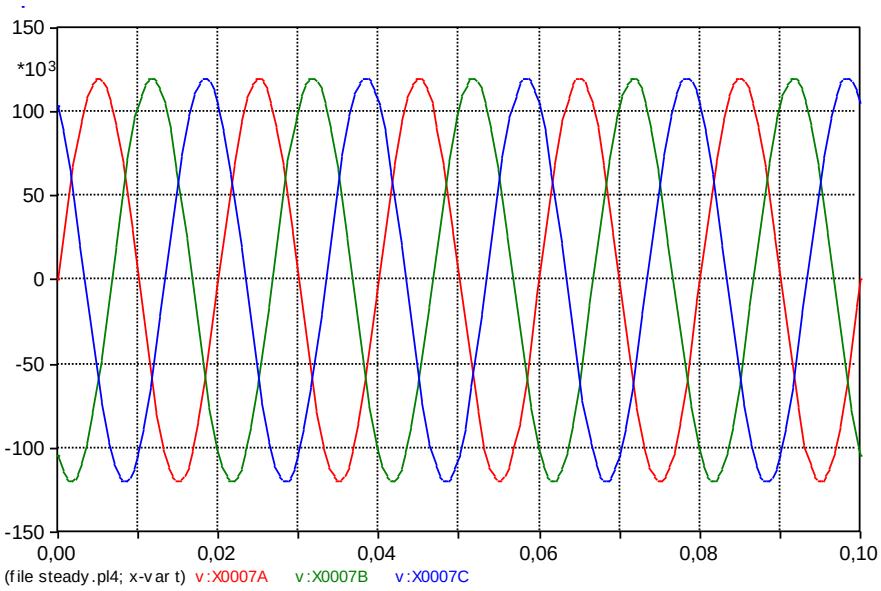

Figure 17: Voltage response on the high voltage side (150 kV) of the transformer (x-axis: time in s; y-axis: voltage in V)

3. The voltage in steady state of the 150 kV infinite grid is depicted in Figure 18. This result is compared with the node-voltage on the high voltage side of the step-up transformer and these are in phase with each other. The peak transformer node-voltage is only a fraction lower than

the peak infinite grid voltage, which is caused by small losses in the HTS circuit (i.e. stray inductances).

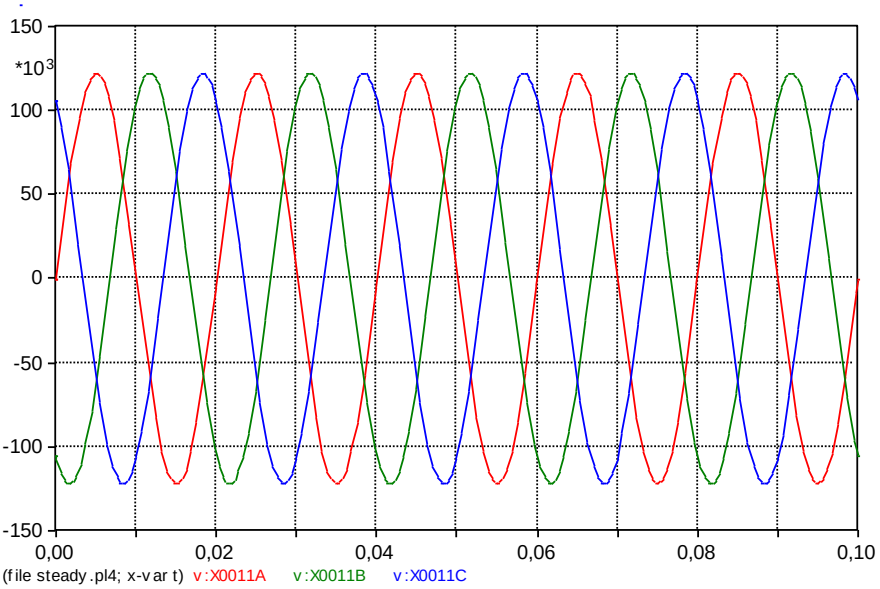

Figure 18: Voltage response of 150 kV infinite grid (x-axis: time in s; y-axis: voltage in V)

From these results it can be seen that the expectations were correct. The different voltages are stable; the signs are proper and the amplitudes are correct.

During the steady-state operation, the current through the FCL HTS cable is very low, compared to a faulted situation. From Figure 19 it can be seen that the non-linear resistance during steady-state is very low (1,11 mΩ) and in accordance with the expectations. This result will be used in succeeding chapters.

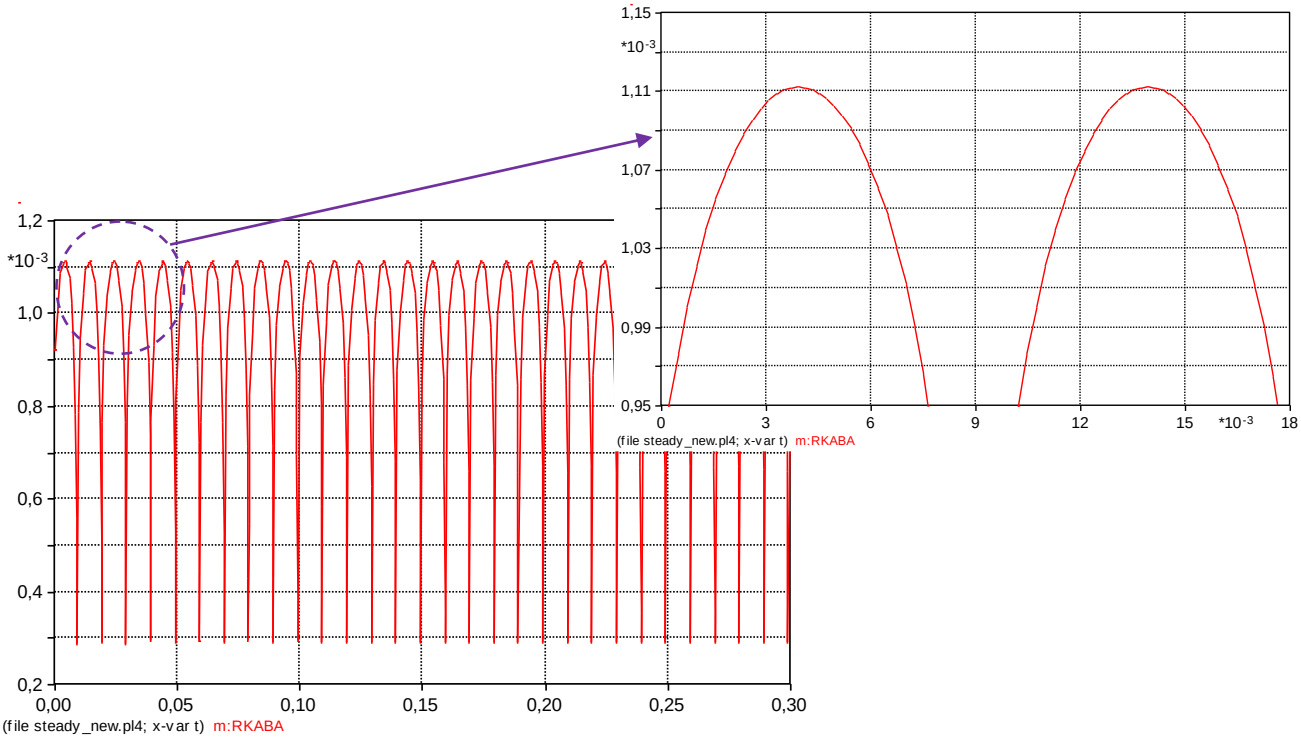

Figure 19: Relation between R and time, during steady-state operation (x-axis: time in s; y-axis: R in Ω)

7. Short-circuit analysis

7.1 Characterization of short-circuits

Any fault in a power system brings the system to an abnormal condition and interferes with the normal flow of power. In practice short-circuit faults are especially of concern, because they result in a switching action [4]. Various types of short-circuit faults can occur in electrical systems (affecting extra-high-voltage-, high-voltage- and lower level voltage systems). These can be caused by all sorts of reasons (5):

- External cause: due to conductor break or hit; accidental contact between two or more conductors, helicopters that accidentally fly on transmission lines, wind and/or ice and digging.
- Breakdown of insulation: due to heat, poor/aged insulation/dielectric, corrosion and/or humidity.
- Internal or atmospheric overvoltage's: due to lightning strokes, switching transients and/or flashovers.

Once a short-circuit fault occurs in a power system, it can have several consequences (for example. electro-dynamic forces, excessive temperature rise in conductors and/or voltage dips.).
In practice different types of short-circuit faults are possible, as depicted in Figure 20-Figure 23.

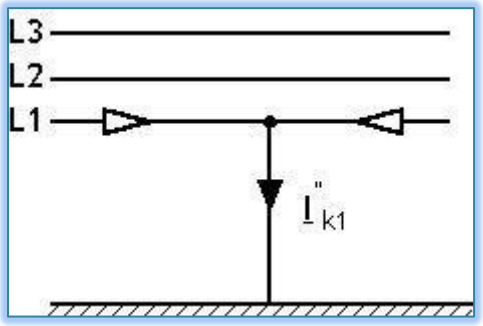

Figure 20: Single line-to-earth short-circuit

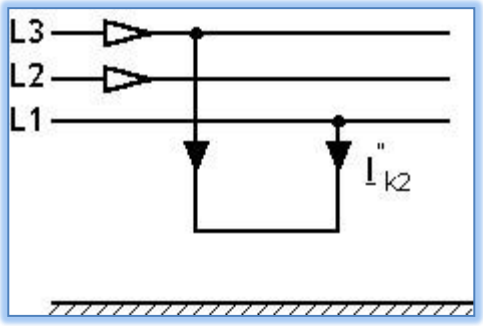

Figure 21: Line-to-line short-circuit

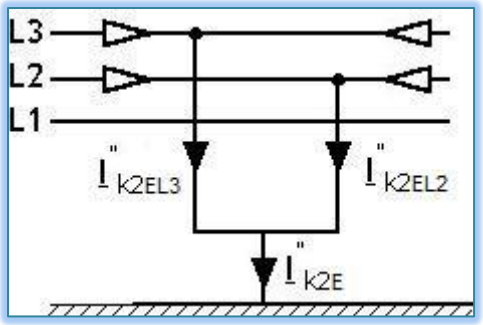

Figure 22: Double line-to-earth short-circuit

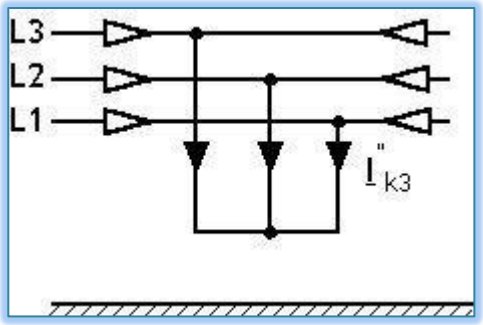

Figure 23: Three-phase short-circuit

Majority of the faults are *single line-to-earth faults* Figure 20 and occur when a conductor (line) touches the earth. *Line-to-line faults* take place when two lines touch each other, as shown in Figure 21. This happens for instance when overhead transmission lines start galloping because of high winds or if a line breaks and falls on a line below. If a conducting path to earth is formed, this becomes a *double-line to earth fault* Figure 22; but this type of fault is very rare.
Three-phase faults (with or without contact with earth) happen when all three lines touch each other or fall to earth [5].
Experience has shown that almost 80% of faults in overhead lines are single-line to earth, 15% line to line and 5% will are three-phase short-circuit faults [4]. In cable networks both multi-line and single-line faults occur but the majority is also single-line to earth.
Even though three-phase faults are very rare, they are the *most severe* faults for the power system and its components. This is also the *main reason* why all the fault analysis in this thesis will be based on *symmetrical three-phase faults*.

All the other types of faults cause an imbalance between the phases, creating *unsymmetrical faults*. In these fault situations the method of symmetrical components based on the Fortescue's theorem is used for analysis of the unsymmetrical faults. Three unbalanced phasors of a three-phase system can be resolved into *three balanced systems* of phasors, containing *positive-sequence-, negative-sequence- and zero-sequence components*. Since symmetrical faults will be studied in this research, going into further details about the unsymmetrical faults is not necessary.

7.2 Peak short circuit currents

When studying short-circuit currents, it is not only important to know what kind of faults can be modeled in a system, but also how to analyze the results of the simulations. In the IEC 60909-0 the following information is given about short-circuit currents, this is used for the analysis of the faults modeled in ATP.

Depending on the location of a fault in a power system, this can be a so-called "near-to-generator short-circuit" (fault location on the terminals of the generator) or a "far-from-generator short-circuit" (fault in the power system). In both cases it is possible to calculate the short-circuit currents which should provide the current as a function of time at the short-circuit location from the initiation of the short-circuit up to its end, corresponding to the instantaneous value of the voltage at the beginning of the short-circuit [5].

The short-circuit currents modeled in this thesis, are based on "far-from-generator short-circuit", see Figure 24, this means that the *DC-component* of the short-circuit current decays fast. The DC-component is an exponential term which describes the relation between the resistance (R) and inductance (L) of a circuit as a function of time: $i_{dc}(t) = \exp\left(-\frac{R}{L}\right)t$.

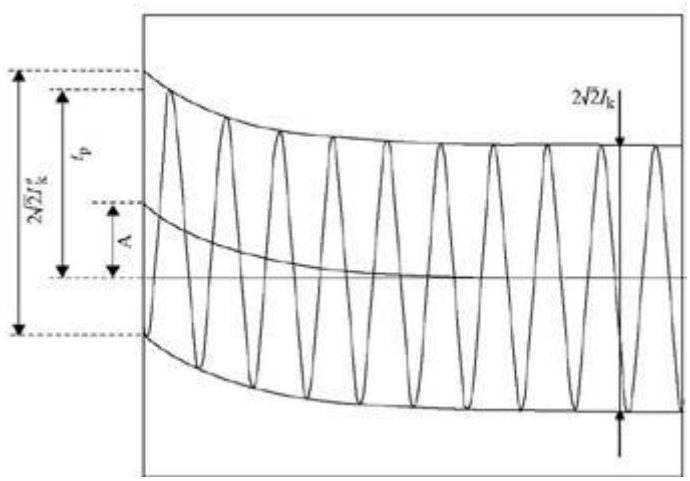

$I_k^{"} = initial\ symmetrical\ short-circuit\ current$

$i_p = peak\ short-circuit\ current$

$I_k = steady-state\ short-circuit\ current$

$i_{d.c.} = d.c.\ component\ of\ short-circuit\ current$

$A = initial\ value\ of\ the\ d.c.\ component\ i_{d.c.}$

Figure 24: Short-circuit for a far-from-generator short-circuit

From short-circuit calculations it is interesting to know the r.m.s. value of the symmetrical a.c. component and the peak value i_p of the short-circuit current following the occurrence of a short-circuit. The highest value i_p depends on the time constant of the decaying a-periodic component; the frequency f; and on the ratio R/X or X/R of the short-circuit impedance. The peak value is reached if the short-circuit starts at zero voltage.

The calculation of the three-phase short circuit currents depend on the configuration of the network. In a meshed network there is no easy method to calculate i_p and $i_{d.c.}$, because there are several direct-current (d.c.) time constants.
The three-phase short circuit currents that are analyzed in this thesis are fed from a non-meshed network; therefore the following equations of IEC 60909 are applied for the short-circuit analysis.

For three-phase short-circuits fed from non-meshed networks the contribution to the peak short-circuit current, from each branch can be expressed by:

$$\boldsymbol{i_{pi} = \kappa\sqrt{2}I_k^{"}} \quad [7.1]$$

The factor κ depends on the R/X or X/R ratio and can be obtained from two graphs (appendix A.2) or calculated by the following expression:

$$\boldsymbol{\kappa = 1,02 + 0,98e^{-\frac{3R}{X}}} \quad [7.2]$$

Finally the peak short-circuit current i_p at a short-circuit location F, fed from sources which are not meshed with one another:

$$\boldsymbol{i_p = \sum_i i_{pi}} \quad [7.3]$$

These equations will be applied to analyze the results of the short-circuit current simulations in succeeding paragraphs.

8. Fault studies and results for short-circuit current analysis

8.1 Introduction fault studies

As mentioned previously symmetrical three-phase faults will be carried out in order to analyze the effect of a FCL HTS cable in a power network, during faults.
Three-phase fault short-circuit currents are simulated for the studied network, with and without a superconducting cable. Two options with the superconducting cable are analyzed, a three-phase fault between the infinite grid and the cable and a three-phase fault between the transformer and the cable.
These results are used for analysis of the fault current limiting effect of the superconducting cable. Furthermore the value of the resistance will be used for the TRV-analysis.

The fault studies that are carried out in this research are:

- ***Fault study one: A three-phase fault to earth is simulated between the 150 kV infinite grid and the 150 kV FCL HTS cable:***

  When a three-phase to earth fault occurs the voltage drops to 0 V and current will flow to the point where the fault has occurred. A large part of the current will flow from the 150 kV infinite grid to the fault and a smaller portion of the current will be “provided” by the generator. The latter current will flow through the FCL HTS cable and the value/result of this current is of main interest. This situation is depicted in Figure 25, where it can be seen that a three-phase fault occurs between the 150 kV grid side and the 150 kV FCL HTS cable.

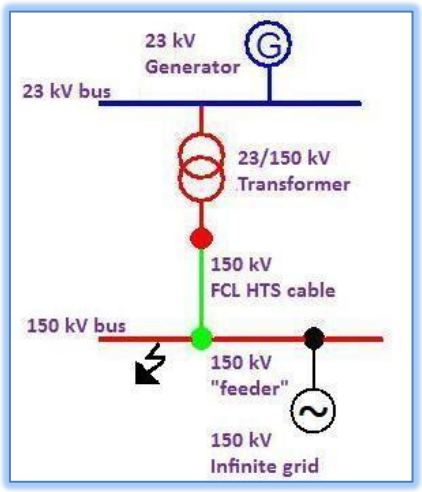

Figure 25: Three-phase fault to earth on the 150 kV infinite grid side

- ***Fault study two: A three-phase fault to earth is simulated between the 23/150 kV transformer side and the 150 kV FCL HTS cable:***

  When this fault occurs the short-circuit current contribution of the 150 kV infinite grid to the fault will flow through the FCL HTS cable. In this case, the current flowing through the cable will be much larger than in the previous case. This situation is depicted in Figure 26, where the fault occurs between the 23/150 kV transformer and the 150 kV FCL HTS cable.

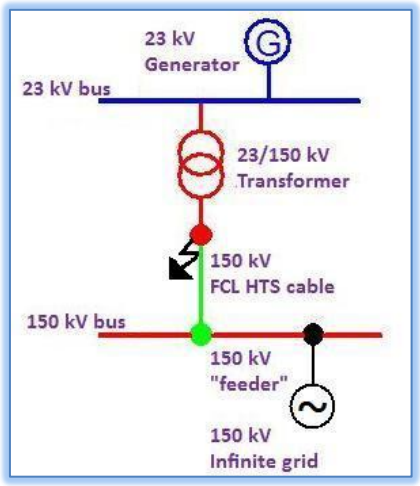

Figure 26: Three-phase fault to earth on the 150 kV transformer side

At last the voltage across the generator terminals is simulated to verify the maximum voltage when the three-phase faults take place. This analysis is important, because exceeding the specified value can be dangerous for the generator windings. Overvoltages can cause insulation breakdown, for example, in generator armature windings.

8.2 Results of the short-circuit current simulations

In the following sub-paragraphs the previously mentioned fault studies will be carried out and simulations will be analyzed. First of all the results of the simulation without the superconducting cable will be presented and afterwards the fault studies are discussed.

8.2.1 Three-phase fault to earth without superconducting cable

The electric circuit depicted in Figure 27 is used to simulate a three-phase fault short-circuit current to earth. In this circuit the non-linear resistive part of the cable is removed, to obtain simulations.

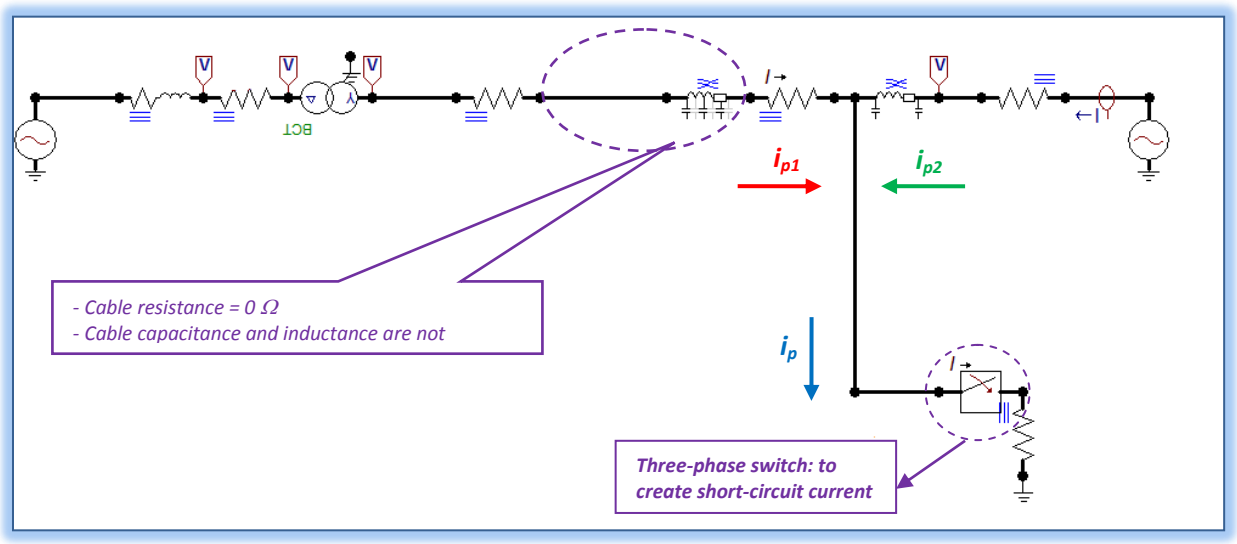

Figure 27: Three-phase fault to earth without superconducting cable

The cable capacitance and inductance stay unchanged and have the same values that are obtained for the superconducting cable, because the non-linear resistive character of the cable varies.

A three-phase switch is used, to simulate a short-circuit fault to earth on t = 100 ms (t = 0 s at the beginning of the simulation). The following short-circuit currents are depicted in Figure 27 :

- i_{p1} = *the peak short-circuit current contributed by the 23 kV voltage source (=generator)*
- i_{p2} = *the peak short-circuit current contributed by the 150 kV (=infinite grid)*
- i_p = *the total network peak short-circuit current*

Figure 28 shows the simulation of a three-phase fault current flowing through the three-phase switch to earth. In this figure the current versus time is plotted for phase A. Further the current decays exponentially with a time constant L/R, which is a constant of the a-periodic term. These results will be used to compare network simulations ***with*** 150 kV FCL HTS cable.

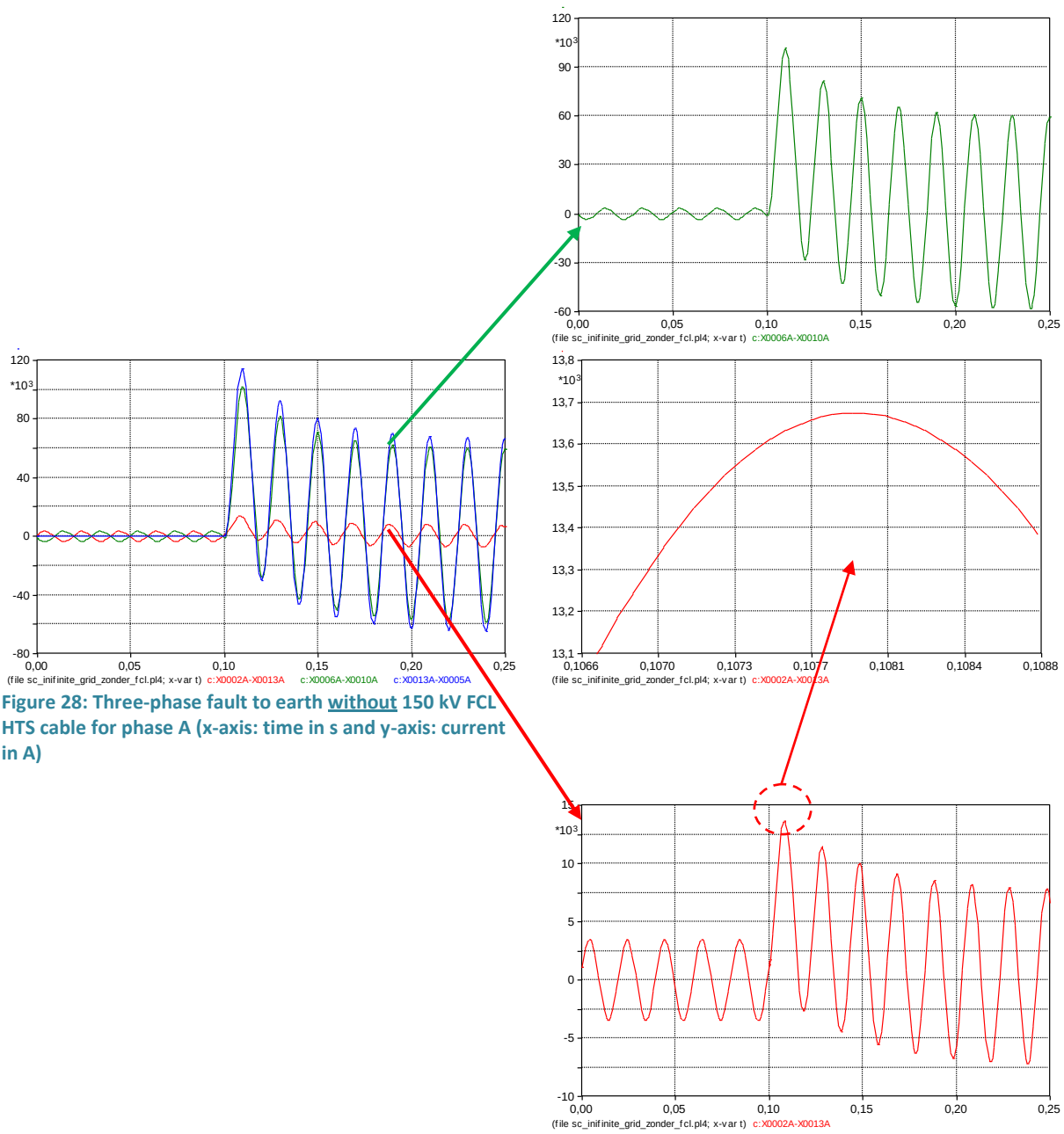

Figure 28: Three-phase fault to earth without 150 kV FCL HTS cable for phase A (x-axis: time in s and y-axis: current in A)

The calculation of the peak fault currents is given in Table 6 (based on the equations of IEC 60909 [7.1]-[7.3]).

calculated peak fault current *)	
peak current	calculated
$i_{p1} = (\kappa * \sqrt{2}) * \left(i_{nom} * \frac{1}{X_d''}\right)$	$(1,746 * \sqrt{2}) * \left(2.10^3 * \frac{1}{0,265}\right) \approx 20\ kA$
$i_{p2} = (\kappa * \sqrt{2}) * I_k''$	$(1,746 * \sqrt{2}) * 40.10^3 \approx 100\ kA$
$i_p = \sum i_{p1} + i_{p2}$	$20\ kA + 100\ kA = 120\ kA$

Table 6: calculated peak fault currents

*) *given by company: R/X-ratio for the infinite grid is 0,1; based on IEC 60909 this means that:* $\kappa = 1,02 + 0,98e^{-0,3} = 1,746$

*) *these peak fault current calculations can only be used if all currents are in-fase, otherwise these values are an approximation*

The peak values of the *calculated* fault currents are compared (in Table 7) with the *simulated* fault currents. The simulated peak values originate from the plots depicted in Figure 28, these peak values are not in-fase, so not on there is some time difference between the peak values.

Compare: simulated and calculated peak fault current		
peak current	calculated (kA)	simulated (kA)
i_{p1}	20	13,7
i_{p2}	100	101,5
i_p	120	114,5

Table 7: peak fault current comparison

From this table the following conclusion can be drawn:

- The (peak) simulated fault current provided by the generator is much lower than the calculated fault current. The difference in this value is acceptable and is mainly caused by the transformer impedance.

The voltage across the generator terminals does not increase the maximum value, as it can be seen from Figure 29.

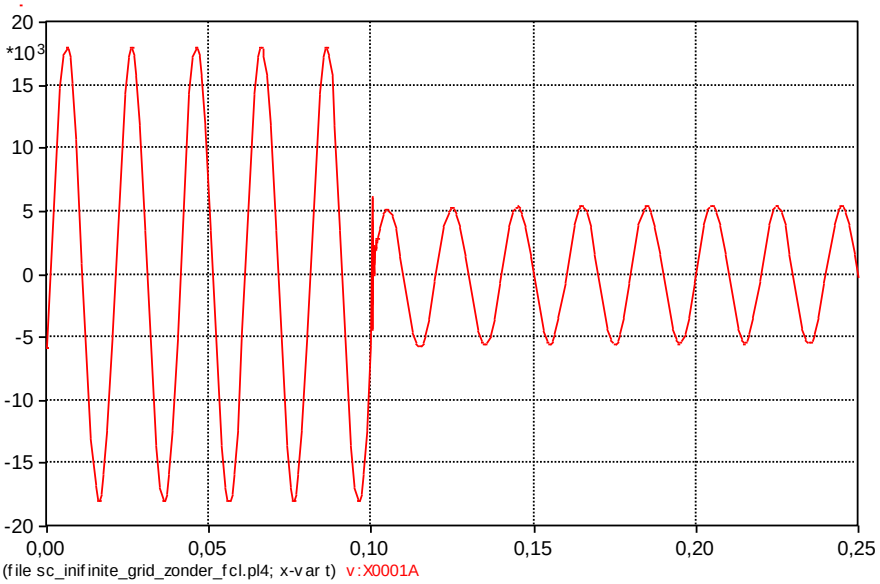

Figure 29: Voltage across the generator terminals, during a fault (without a superconducting cable) (y-axis: voltage in kV; x-axis time in s)

Typical phenomenon of fast switching actions, thus in this case fast current limiting action, is that overvoltages can damage the insulation of other high-voltage components in the power system. In the fault studies the danger could be that overvoltages could damage the generator windings. Though, the expectation is that this will not be the case for the fault simulations with FCL HTS cable.

8.2.2 Three-phase fault to earth simulated between the 150 kV infinite grid and the 150 kV FCL HTS cable

In this fault study a three-phase fault to earth is created between the FCL HTS cable and the 150 kV voltage source (= 150 kV infinite grid), to investigate the dynamic short-circuit current withstand of the generator. This is done by using a three-phase switch and creating a short-circuit to earth on t = 100 ms (t = 0 s at the beginning of the simulation).
The expectation is that a large amount of current will flow from the 150 kV voltage source (= 150 kV network) to the point of fault. A smaller amount of current will flow from the 23 kV supply (= 23 kV generator) through the FCL HTS cable to the point of fault. The fault current limiting effect of this cable, should limit the fault current when the current becomes higher that the defined critical current (3,67 kA). As it was seen in the simulations without a FCL HTS cable, the short-circuit current flowing from the generator is significantly higher than the critical current. For this reason a limitation of the fault current is expected.

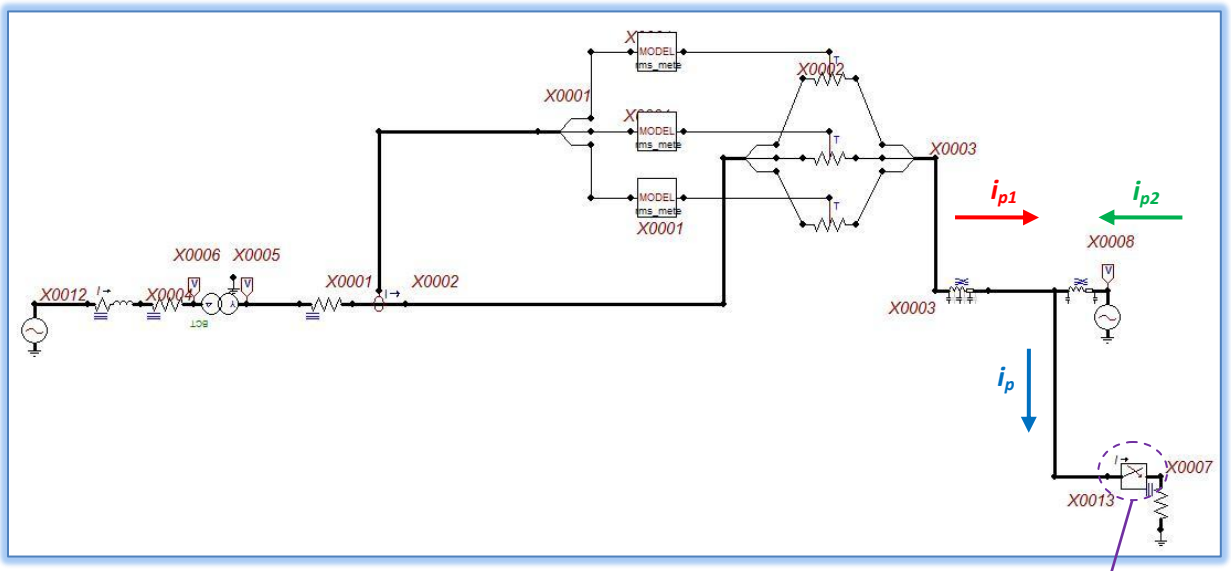

Figure 30: Three-phase fault to earth on the 150 kV infinite grid side of the FCL HTS cable

In Figure 30, the ATP model for this case is depicted with the 150 kV FCL HTS cable. The SWIT_3XT ATP three-phase switch is used to simulate the three-phase short-circuit. The impedance that is connected between the three-phase switch and earth is very small (R = 1e-6 Ω). The contribution to the three-phase fault current from each branch, is drawn in Figure 30, see the colored arrows:

- i_{p1} = *the peak short-circuit current contributed by the 23 kV voltage source (=generator)*
- i_{p2} = *the peak short-circuit current contributed by the 150 kV (=infinite grid)*
- i_p = *the total network peak short-circuit current*

Figure 31 shows the simulation of a three-phase fault current flowing through the three-phase switch to earth. In this figure the current versus time is plotted for phase A.

In the pre-fault situation (before t = 100 ms) the currents are in steady-state and in-fase; after that instant, the fault is simulated and oscillations occur. This pattern of the short-circuit can be recognized from other literature or IEC 60909 (50 Hz short-circuit current decaying with a non-periodic term).

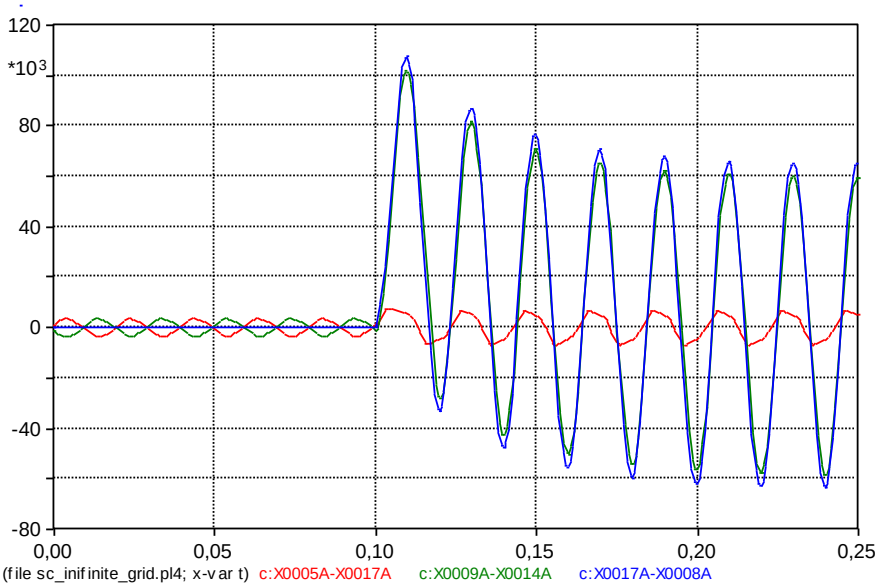

Figure 31: Three-phase fault to earth between the 150 kV infinite grid and the 150 kV FCL HTS cable (x-axis: time in s and y-axis: current in A)

The simulated “red current” is the fault current that is provided by the 23 kV generator, thus the fault current flowing through the 150 kV FCL HTS cable. It is therefore interesting to further investigate this fault current and compare the results with the simulations without a superconducting cable.
It is visible that red-current (coming from the generator and in this case limited by the FCL HTS cable) has a low a-periodic term and is not in-fase with the other currents. This is caused by the dominating non-linear resistance of the FCL HTS cable (as will be seen in the following figures). Due to the increase of the non-linear resistance the L/R-ratio (a-periodic term) has decreased.

In Figure 32 and Figure 33 the three-phase fault current simulations without 150 FCL HTS cable and with 150 kV FCL HTS cable, respectively, are compared. As it can be seen from these graphs the fault current is reduced by **6,01 kA$_{peak}$**.
The dominating non-linear resistance does not only limits the fault current, but also changes the sinus.

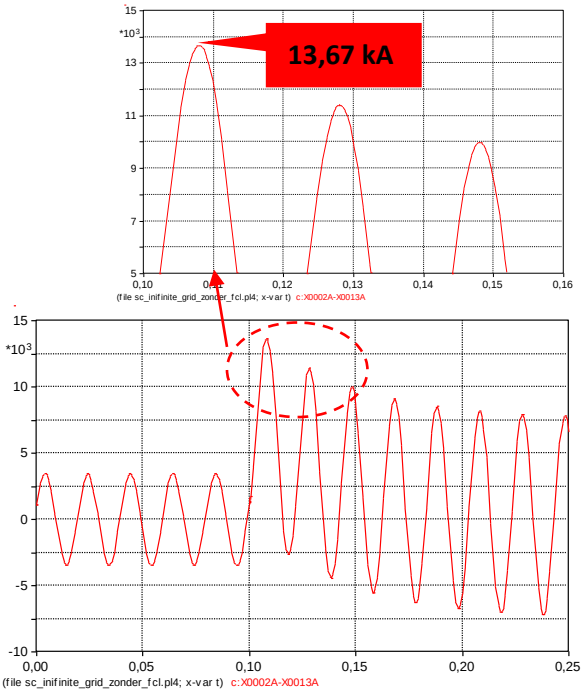

Figure 32: : Three-phase fault to earth **without** 150 kV FCL HTS cable for phase A (x-axis: time in s and y-axis: current in A)

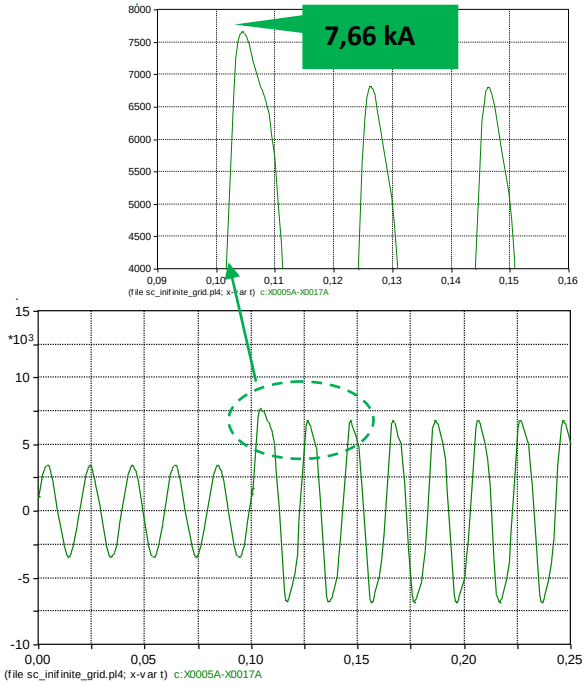

Figure 33: : Three-phase fault to earth **with** 150 kV FCL HTS cable for phase A (x-axis: time in s and y-axis: current in A)

In Figure 34 the non-linear resistance is depicted as a function of time. It obvious that the non-linear resistance is very low before the fault is simulated, because the cable is in the superconducting state. From what is known about the physical behavior of the superconducting cable, it is expected that when the critical current (I_c) starts flowing through the FCL HTS cable a transition takes place in the cable. The superconducting state of the cable decreases and the resistance increases non-linearly. For the type of superconducting material that is used for this research, the highest value of the resistance becomes in this case slightly higher than 10 Ω, at the maximum value of the fault current and around 6 Ω, during steady-state value of the fault current. These values are marked in the plots of Figure 34 and will be used for the TRV analysis.

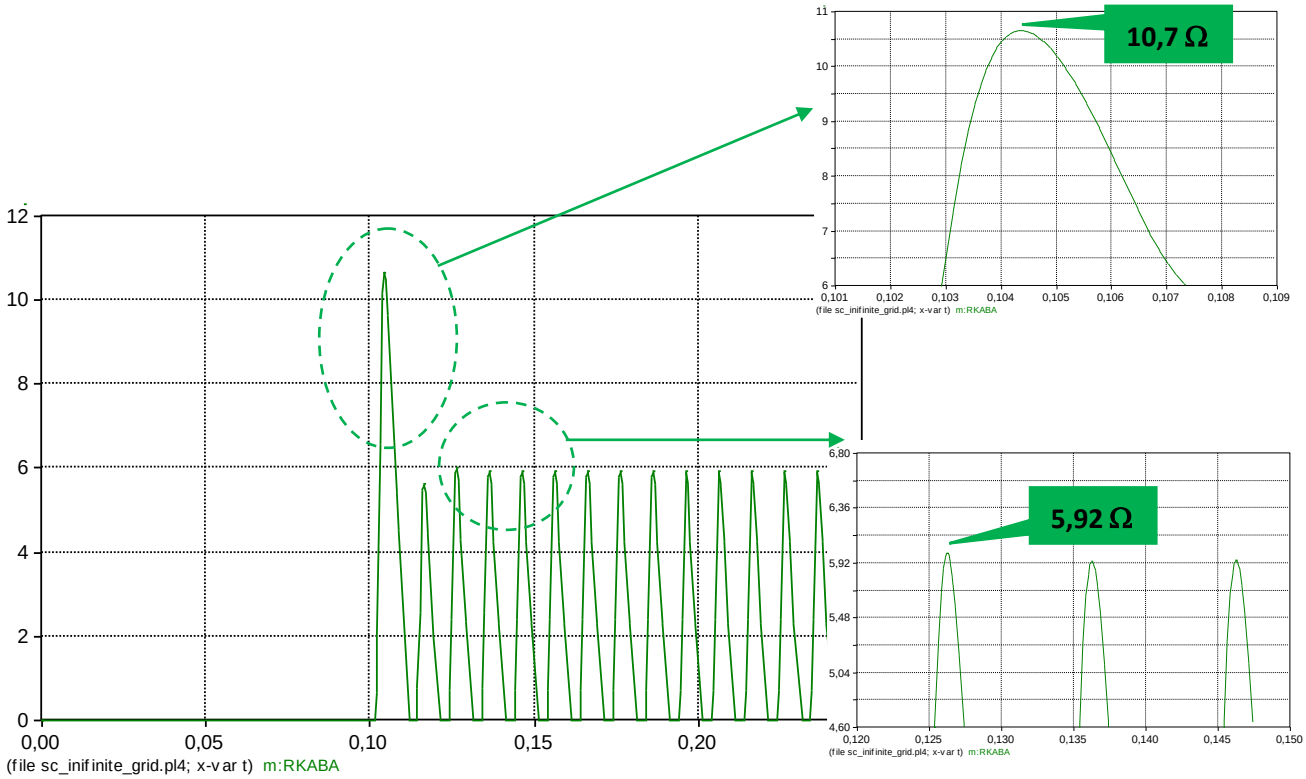

Figure 34: Non-linear resistance of 150 kV FCL HTS cable as a function of time, during a fault between cable and infinite grid (y-axis: non-linear resistance in Ω; x-axis: t in s)

Finally the voltage across the generator terminals, at the moment of the fault, is simulated in Figure 35. It can be seen that the voltage across the generator terminals is lower at the moment of the fault. Hence there is no danger for the generator windings and insulation.

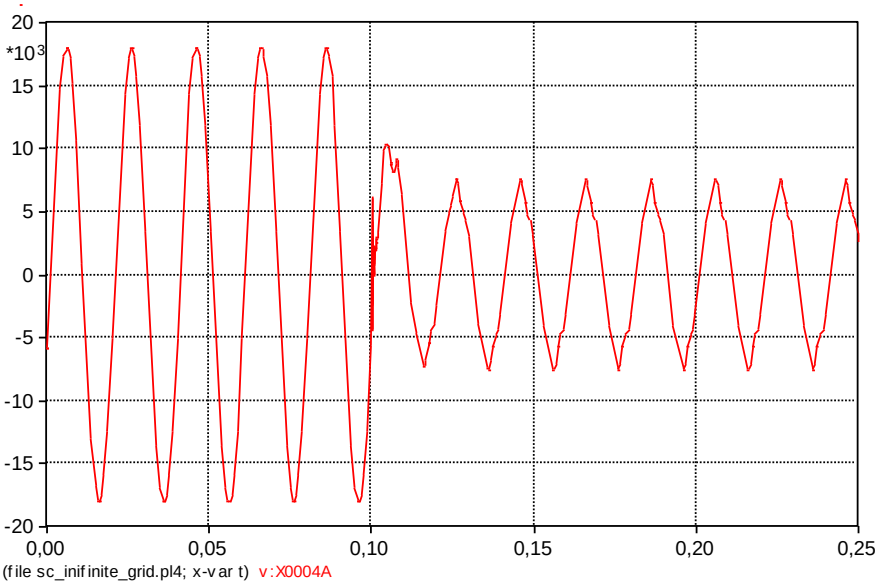

Figure 35: Voltage across the generator terminal, during a fault between cable and infinite grid (y-axis: voltage in kV; x-axis: t in s)

8.2.3 Three-phase fault to earth simulated between the 23/150 kV transformer and the 150 kV FCL HTS cable

For this fault study a fault is created between the 23/150 kV transformer and the 150 kV FCL HTS cable. Compared with the previous fault study a larger amount of short-circuit current will flow through the FCL HTS cable, because the short-circuit current contribution from the 150 kV voltage source will flow through this cable to the fault location. The value of the fault current, flowing through the FCL HTS cable, will exceed the *critical current* (I_c) specified for the cable. The remaining part of the fault current will be contributed by the 23 kV supply (= 23 kV generator).

In the following figures the circuit and results of this fault study will be presented and analyzed.

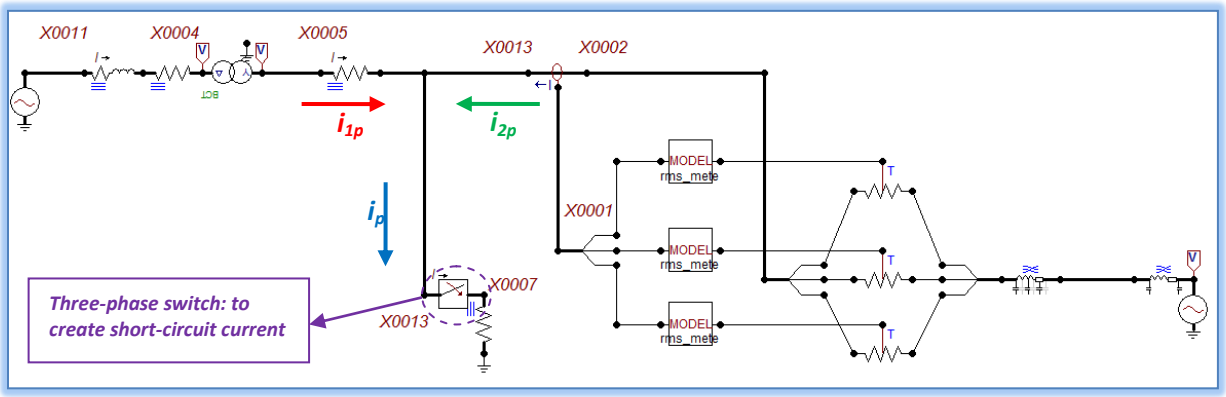

Figure 36: Three-phase fault to earth on the 150 kV transformer side of the FCL HTS cable

Basically, this fault study will be done in the same way as the previous case, at t = 100 ms a three-phase fault to earth is simulated. This is done by applying a three-phase switch in the model and creating a fault to earth Figure 36. The impedance that is connected between the three-phase switch and to earth is very small (R = 1e-6 Ω). The fault current simulation of all the peak fault currents and generator terminal voltage will be depicted in the annexes (A.3).

In this fault study the simulation ***without*** a 150 kV FCL HTS cable will once again be compared with the simulation ***with*** a 150 kV FCL HTS cable. In this, during a fault, a larger amount of the short-circuit current will flow through the 150 kV FCL HTS cable.

The results of these two simulations are depicted in Figure 37 and Figure 38; the first simulation is ***without*** a 150 kV FCL HTS cable and the second simulation is ***with*** a 150 kV FCL HTS cable for phase A. It can be seen from the graphs, the peak short-circuit current is roughly 10 times lower **with** a FCL HTS cable. Once again the L/R-ratio has decreased, due to the dominating non-linear resistance.

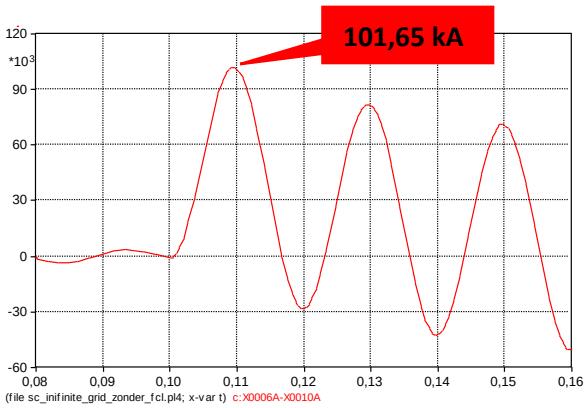

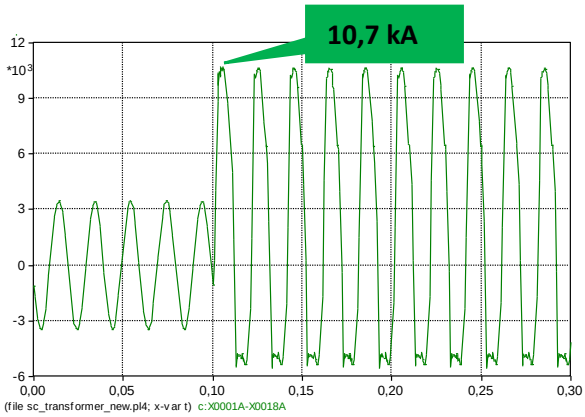

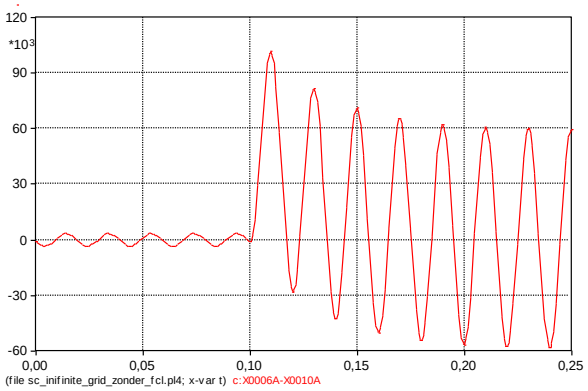

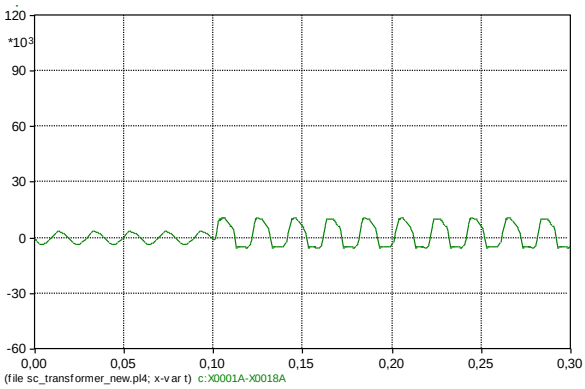

Figure 37: Three-phase fault to earth *without* a 150 kV FCL HTS cable for phase A (x-axis: time in s and y-axis: current in A)

Figure 38: Three-phase fault to earth between the 23/150 kV transformer *with* a 150 kV FCL HTS cable for phase A (x-axis: time in s and y-axis: current in A)

From these results can be concluded that by using a FCL HTS cable, the peak short-circuit current decreases from roughly 100 kA to 10,7 kA (peak value). This is very advantageous for the dynamic short-circuit withstand, because the fault current is reduced to an acceptable value for components (i.e. circuit breaker) in the power system.

In the first fault study the total fault current limitation was **6 kA** when comparing the momentary peak fault currents ***without*** and ***with*** superconducting cable. **This was of major interest, because the total short-circuit current withstand has decreased**.

It can be seen from the results of the second fault study that the momentary peak fault current is limited by a factor 10. The total fault current limitation is **90 kA (≈ 100 kA – 10 kA)** when comparing the momentary peak fault currents ***without*** and ***with*** superconducting cable.

This result satisfies the expectations, the larger the momentary peak fault currents become, the faster the non-linear resistance of the FCL HTS cable increases. Consequently, this means that the momentary peak currents are reduced by 90% when a FCL HTS cable is implemented (side effect, because the first fault study is the major interest).

Higher instantaneous peak fault currents result into, faster increase of the non-linear resistance of the FCL HTS cable.

Subsequently, in this fault study the non-linear resistance as a function of time is depicted in Figure 39. As it has been seen in the previous fault study, the non-linear resistance is very low before the fault.
When the value of the momentary peak current exceeds the critical current (I_c), a transition takes place in the FCL HTS cable. The superconducting state of the cable decreases and the resistance increases non-linearly. For this fault study the non-linear resistance is 55 Ω, at the maximum peak value and is marked in the Figure 39. This result will be applied for the TRV analysis.

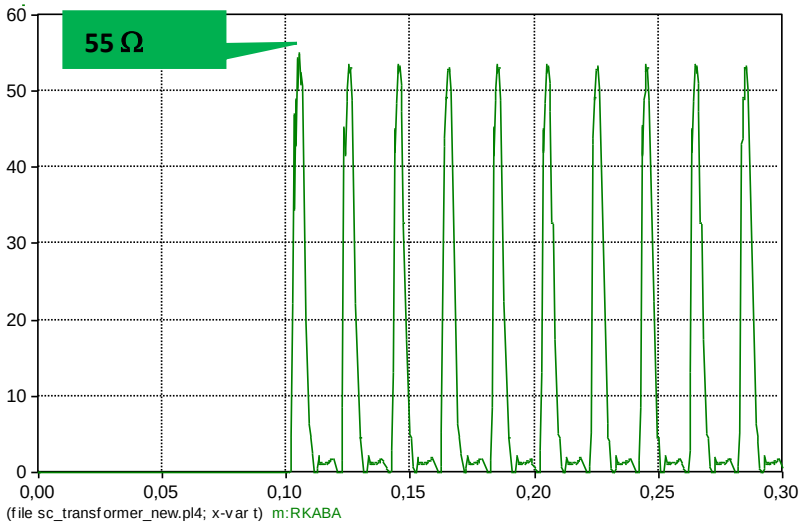

Figure 39: Non-linear resistance of 150 kV FCL HTS cable as a function of time, during a fault between cable and transformer (y-axis: non-linear resistance in Ω; x-axis: t in s)

Finally the voltage across the generator terminals, at the moment of the fault, is simulated in Figure 40. It can be seen that the voltage across the generator terminals is lower at the moment of the fault.

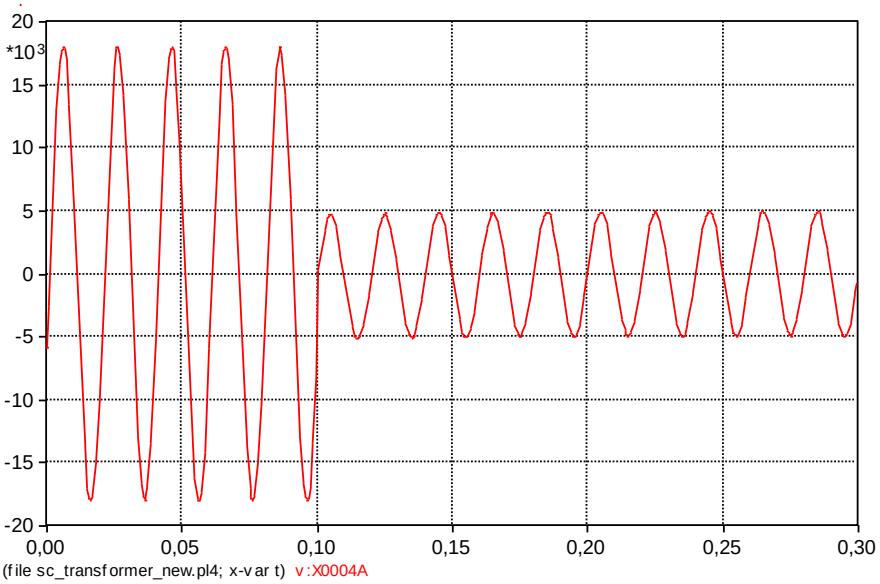

Figure 40: Voltage across the generator terminal, during a fault between cable and transformer (y-axis: voltage in kV; x-axis: t in s)

9. Transient Recovery Voltage

9.1 Fundaments of transient analysis

When a three-phase fault is cleared the power system changes from a steady-state situation, in which the three-phase short-circuit current is flowing, to the state in which only the power frequency-recovery voltage is present [6]. In general a fault in a power system is cleared by parting the contacts of a circuit breaker. Across the open contact an overvoltage is developed and this overvoltage is called ***T**ransient **R**ecovery **V**oltage (TRV)* of the circuit breaker.
The TRV is considered to be composed of an alternating component of 50 Hz and an oscillatory component with exponential delay. The ***r**ate of **r**ise of the **r**ecovery **v**oltage (RRRV)* is an important parameter in the power system operation and is specified in kilovolts per microsecond (kV/μs) in IEC 62271-100.

The TRV is caused by oscillations that take place in the power system, due to the interruption of a short-circuit current. During the fault there is still magnetic energy stored in several inductances (component-, leakage and self-inductance) of the power system and a sudden change in such a dominating inductive circuit always involves a transient. Propagating electromagnetic waves through the system are the cause of transient overvoltages.

This research thesis is not about circuit-breakers, but the fundamental principles of this interrupting device are used to explain the behavior of transients in the studied network.

The FCL HTS cable is used to limit a fault current, in case of a short-circuit in the studied network. This physical behavior of the FCL HTS cable causes transient in the power system, because a sudden change takes place in the circuit.

Similarity and difference between circuit-breaker and FCL HTS cable

The **similarity** between circuit-breakers and FCL HTS cables is that both components are used in power circuits to decrease fault currents. In both cases transients arise in the power system due to their current interaction in the circuit.

The **difference** between these components is the way of reducing a fault current in a circuit. It is obvious that a circuit-breaker completely clears a fault current (considering proper functioning) and a FCL HTS cable limits a fault current until a certain value.
In a circuit-breaker a resistive-arc arises when the contacts separate, causing a thermo-dynamic process (due to arc-plasma) in the component. Regarding a FCL HTS cable a transition takes from the superconducting to the normal state, the so-called quench. The cable is self triggering without either detecting or active triggering mechanism. In case of a circuit breaker protection relays are used for triggering.

In order to analyze the TRV that will appear when fault currents are limited, two different approaches will be used. These are based on the functionality of circuit breakers:

- First approach: the first method is based on an ***arc-circuit interaction*** that is described by Prof. ir. Sluis in the book "Transients in Power Sytems" on pages 74-76. (explained in the appendix)

- Second approach: the second method an ***arc-model*** that is programmed in MODELS and is based on ***modeling of a circuit breaker arc*** and estimation of RRRV.

Both methods are based on the principles of circuit breakers. To have the rate of rise of recovery voltage (RRRV) estimated accurately, it is important to know the value of the resistance of the cable. The influence of the change in resistance will become clear when the results of the simulations will be discussed.

9.2 Black box circuit breaker arc-model

Depending on the purpose of modeling switching arcs, these can be described by three models:

- Physical models

- Black box models (also often called P-τ models)

- Parameter models

Physical arc models are to design circuit breakers and develop new prototypes. These models consist of many differential equations, which are based on fluid dynamics. The Laws of Thermodynamics in combination with Maxwell's equations are obeyed by the physical arc models.

The ***black box switching or circuit breaker arc models*** are based on the behavior of the arc, rather than on the physical processes. These models are not suited to design circuit breaker interrupters, but are useful mathematical models to simulate the interaction between an arc and electrical network in transient studies. The behavior of the arc is described by simple mathematical equations, which are derived from the relation between the arc conductance and measurable parameters (arc voltage and current).

Parameter models are a complex variation of black box models. Sophisticated functions and tables are used for the essential parameters of the black box model.

The well-know classical ***black box models*** that are used for transient analysis are the *Cassie model* and the *Mayr model*. The equations of these models are a solution of the *general arc equation*. In the general equation of the black box model, the arc conductance is defined as a function of the electrical power input to the plasma channel; heat dissipation in the plasma channel; and the time:

$$g = F(P_{in}, P_{out}, t) = \frac{i_{arc}}{u_{arc}} = \frac{1}{R} \quad [9.1]$$

with

g	= momentary arc conductance
P_{in}	= power input to the plasma channel
P_{out}	= power transported from plasma channel: power input minus heat dissipation
t	= time
i_{arc}	= momentary arc current
u_{arc}	= momentary arc voltage
R	= momentary arc channel resistance

As can be seen in equation [9.1] the momentary arc conductance changes if the input and output power are not in equilibrium.

The momentary arc conductance can be expressed as a function of the energy stored in the plasma channel:

$$g = F(Q) = F\left[\int_0^t (P_{in} - P_{out})dt\right] \quad [9.2]$$

Eventually the change of the arc conductance is defined by the general arc equation:

$$\frac{1}{g}\frac{dg}{dt} = \frac{d[ln\,(g)]}{dt} = \frac{F'(Q)}{F(Q)}(P_{in} - P_{out}) \quad [9.3]$$

In order to solve this general arc equitation, some assumptions have to be made. Different solutions are available and these are named after the researchers of the different black box models.

The general arc equation is used to program an ATP-MODELS component [6], to simulate a transient that would occur in the network when a fault current is limited. The steady state power of the arc, peak value of the current, arc time constant and the separation time of the circuit breaker are defined as data in MODELS (see Table 8).
The separation time of the circuit breaker is very small, in the order of micro-seconds. It is a challenge to plot sufficient points in ATP-plot in such a short time. This means, that if a circuit is built, a MODEL file is programmed and all together the total ATP file "runs", the results of the plots are sometimes still not useful. If there are not enough plotting points, it is not possible to calculate the *du/dt* of the TRV correctly.

DATA	UNIT	VALUE	SYMBOL
steady state **arc-power**	MW	0,2	
i_{max}: peak of the sine wave in the circuit breaker	kA	40	
τ: arc-time constant	μs	40	
contact **separation time**	s	0,005	
INPUT		current (A)	
OUTPUT		arc-resistance (Ω)	
OUTPUT		switch commando (open or close)	
ATP SIMULATION SETTINGS: time domain			
DATA PARAMETER	**UNIT**	**VALUE**	
delta_T	s	5.10^{-9}	
Tmax	s	0,008	

Table 8: Data-parameters for MODELS_black box arc model

Further, the current of the circuit is an input and is used to calculate the arc conductance. Depending on the value of the arc conductance the contacts of the circuit breaker open or stay closed. Combining this arc model with the network that is used to calculate shot-circuit currents and the effective value of the resistance, the *du/dt* of the TRV can be calculated. The network that is used to simulate the TRV is depicted in Figure 41.

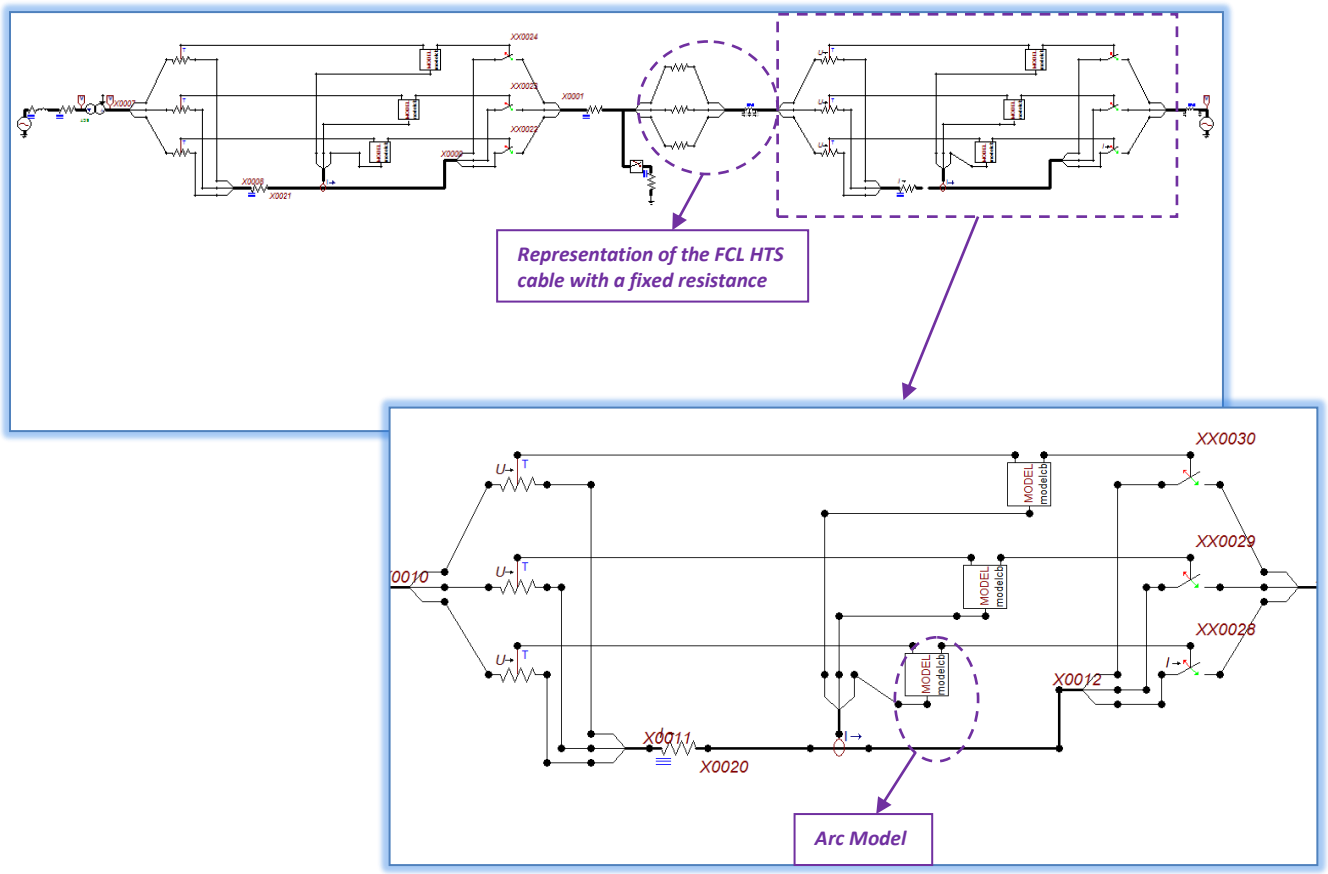

Figure 41: Complete system to calculate du/dt

Basically, this is the same circuit that was used to simulate three-phase fault currents. Now an Arc Model of a circuit breaker is applied to quench the short-circuit current, when a fault is simulated. This is done to imitate the process of fault current limitation of the FCL HTS cable. For this imitation two resistance values of the FCL HTS cable have been used; these values where calculated during the simulations of the three-phase fault current in the fault studies.

On a certain moment the circuit breaker is triggered to switch off the fault current, by opening the breaker contacts. If the circuit breaker works properly the short-circuit current is interrupted at current zero, as can be seen in Figure 42. The fault current flowing through phase B is the first fault current that is cleared (green line in Figure 42). Considering this, the expectation is that the TRV will appear on phase B.
When zooming in on the current-zero, a so called post-arc current flows after current zero. The magnitude and duration of the post-arc current depend on the parameters of the circuit and the design of the circuit breaker. The value of the post arc current may or may not be sufficient to modify the shape of the TRV.

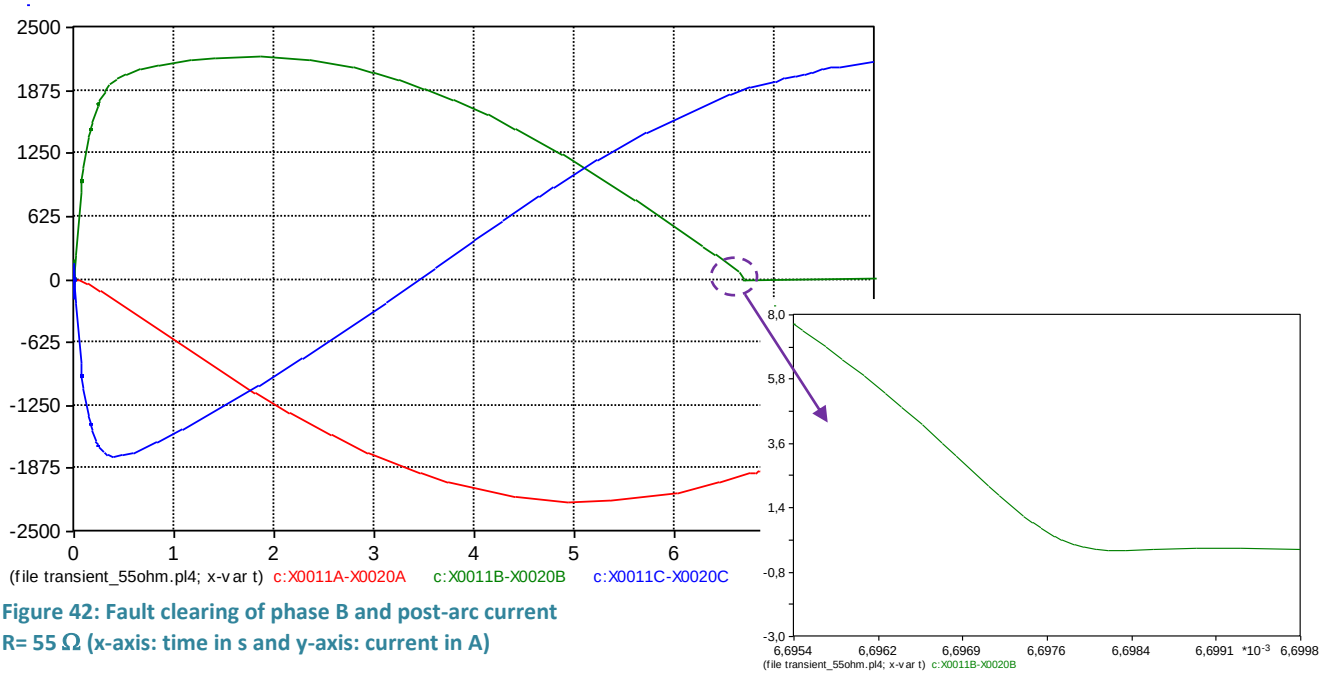

Figure 42: Fault clearing of phase B and post-arc current R= 55 Ω (x-axis: time in s and y-axis: current in A)

The next step is to plot the voltage simulations of all three-phases. As mentioned before, the prospect is that the TRV will appear in phase B, the voltage response of all three-phases is depicted in Figure 43. The gridlines are removed, so that it is visible that the TRV appears in phase B (green line in Figure 43).

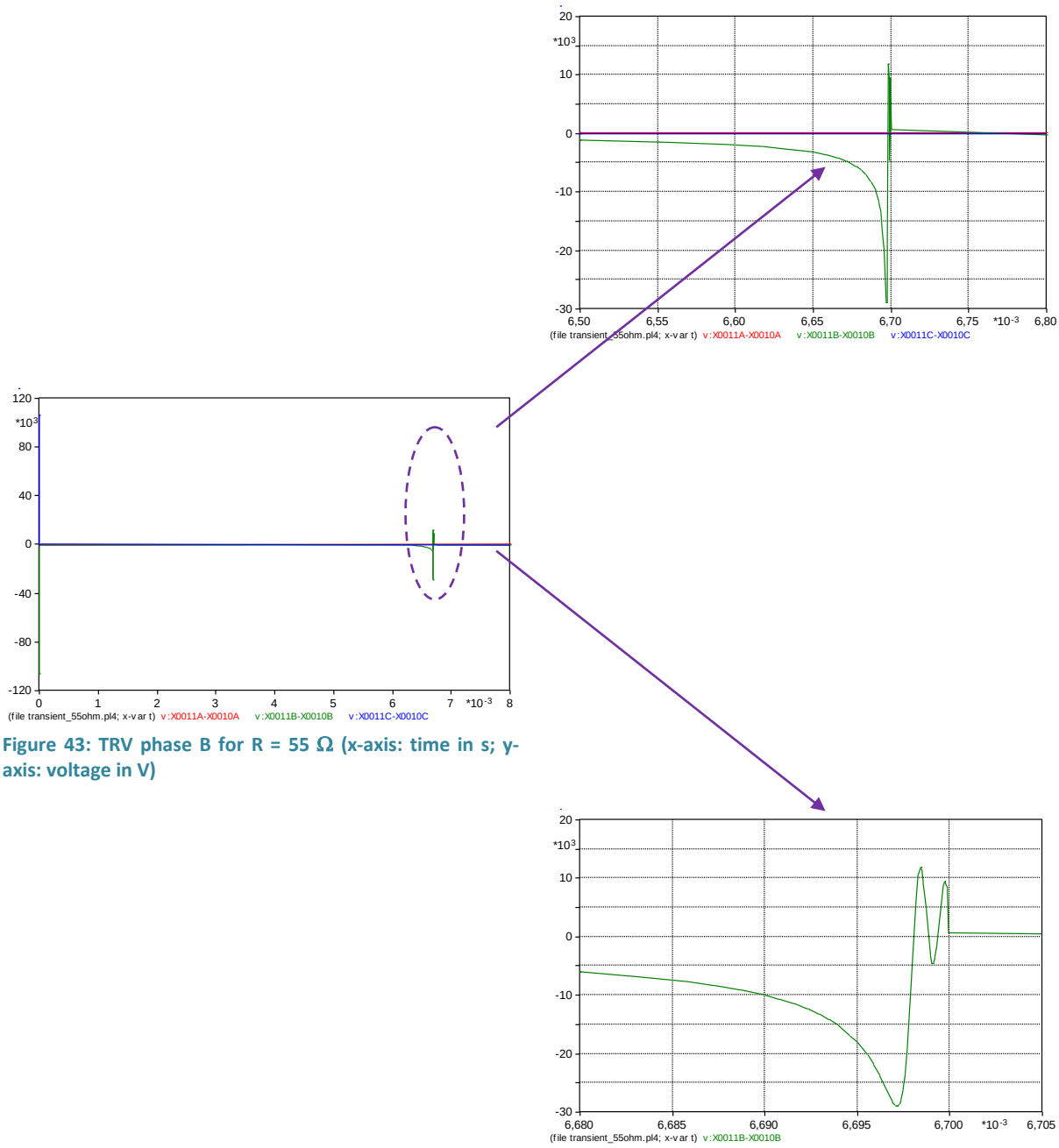

Figure 43: TRV phase B for R = 55 Ω (x-axis: time in s; y-axis: voltage in V)

In Figure 43 the overvoltage that arises after the circuit breaker of phase B is opened, is depicted. By using this plot, two points are chosen to calculate the steepness (du/dt) of the TRV. The result of this calculation is given in Table 9.

R = 55Ω			
Time [ms]		**Voltage [V]**	
t1	6,6981	u1	5581,5
t2	6,6982	u2	5809,4
Δt	0,1	Δu	227,9
	$\frac{du}{dt} = \frac{u2-u1}{t2-t1} = 2279\frac{V}{ms} = 2,3\frac{kV}{us}$		

Table 9: Results of TRV in phase B, when R = 55 Ω

As can be seen from these results the *du/dt = 2,3 kV/μs*. This RRRV is verified with the standard value that is allowed, based on IEC 62271-100.

For this comparison IEC test duty T10 is used, because the maximum fault current (2,5 kA green line in **Error! Reference source not found.**) is about 4 percent of the nominal short-circuit current (40 kA).

The standard TRV parameters are grouped for certain values, being 10%, 30%, 60% and 100% of the maximum short-circuit current rating for the specified voltage level of 245 kV. In the IEC standards, these current values are referred to as test duties and the corresponding TRV parameters are tabled for these duties [6].

For test duty T10 12,6 *kV/μs* is the maximum RRRV that is allowed for a nominal voltage rating of 100 kV and above. This means that the *du/dt = 2,3 kV/μ* (for this calculation) is within the limits based on the requirements of the standard.

Proceeding with the same method of RRRV calculation, the identical steps are done for R = 10 Ω and 5,9 Ω. The results are shown in Table 10 and Table 11.

R = 10 Ω			
Time [ms]		**Voltage [V]**	
t1	7,4705	u1	3484
t2	7,4706	u2	3876,3
Δt	0,1	Δu	392,3
	$\frac{du}{dt} = \frac{u2-u1}{t2-t1} = 3923\frac{V}{ms} = 3,9\frac{kV}{us}$		

Table 10: Results of TRV in phase B, when R = 10 Ω

For this simulation the *du/dt = 3,9 kV/μs*. Comparing the RRRV with the standard value that is allowed by the IEC the calculation fulfills the required value. For this case IEC test duty T30 is used, because the maximum fault current (10 kA) is about 25 percent of the nominal short-circuit current.

For test duty T30 5 *kV/μs* is the maximum RRRV that is allowed for a nominal voltage rating of 100 kV and above. This means that the *du/dt = 3,9 kV/μ (*for this calculation) is within the limits based on the requirements of the standard.

R = 5,9 Ω			
Time [ms]		**Voltage [V]**	
t1	7,9722	u1	43344
t2	7,9723	u2	43902
Δt	0,1	Δu	558

$$\frac{du}{dt} = \frac{u2 - u1}{t2 - t1} = 5580 \frac{V}{ms} = 5,6 \frac{kV}{us}$$

Table 11: Results of TRV in phase B, when R = 5,9 Ω

For this simulation the *du/dt = 5,6 kV/μs*. Comparing the RRRV with the standard value that is allowed by the IEC the calculation fulfills the required value. For this case IEC test duty T60 is used, because the maximum fault current (18 kA) is about 45 percent of the nominal short-circuit current.

For test duty T60 3 *kV/μs* is the maximum RRRV that is allowed for a nominal voltage rating of 100 kV and above. This means that the *du/dt = 5,6 kV/μ (*for this calculation) is not within the range, based on the requirements of the standard.
For this exceeding value more investigation is necessary, this is not done in this research.

Conclusions

The main goal of this research is to analyze the effect of a 150 kV Fault Current Limiting High Temperature Superconducting cable, if a new generator is connected to the power network. Important assumptions that have been are the cooling of the cable, due to thermal losses, should not be a problem; and that the studied cable is homogenous throughout its whole length of 300 m. For the analyses it was assumed that enough cable data information and a non-linear characteristic for the resistance versus current would be available. On the contrary, the literature research revealed that there was only cable data available for lower voltage levels. Using these data an approximation has been made for the non-linear characteristic and is based on first generation superconducting tapes. This was the most time-consuming part of the research.

After defining the cable parameters a working model was developed in MODELS of ATPDraw. This cable model was inserted in a 150 kV power network (in ATPDraw). Whereupon two fault studies were defined to carry out three-phase short-circuit current analysis and Transient Recovery Voltage analysis.

The two simulations of the three-phase fault current studies have been compared with a simulation without a FCL HTS cable.

For the first fault study a fault was created between the 150 kV infinite grid and the 150 kV FCL HTS cable. This study has shown that the three-phase short-circuit current flowing to earth at the fault place, is contributed by the 23 kV and 150 kV voltage source, respectively a new 23 kV generator plant and the 150 kV infinite grid. The major contribution to the three-phase fault current is coming from the 150 kV infinite grid. The scarce portion coming from the 23 kV voltage source, flows through the 150 kV FCL HTS cable. The latter current is limited by the 150 kV FCL HTS cable, from 13,7 kA_{peak} (***without*** superconducting cable) to 7,6 kA_{peak} (***with*** superconducting cable). The limited generator current has a low a-periodic term and the fault current is not in-fase with the other currents, this is caused by the dominating non-linear resistance of the FCL HTS cable.
The voltage across the terminals of the generator are within the limits, at the moment of fault. These results satisfy the main goal of the research.

In the second fault study a fault is created between the 23/150 kV transformer and 150 kV FCL HTS cable. The fault current that should be limited is provided by the 150 kV infinite grid. For this case the is limited by the 150 kV FCL HTS cable, from 101,7 kA_{peak} (***without*** superconducting cable) to 10,7 kA_{peak} (***with*** superconducting cable). This is an extra result which shows, that a limitation of 90% of the current is possible and is caused by the non-linear resistance of the cable. The L/R-ratio of this current is lower than in the previous case, this effect is once again caused by the non-linear resistance of the cable.

In order to do TRV analysis two different approaches are used, which compare the functionality and principles of a circuit breaker with the fault current limiting effect of the FCL HTS cable. The first method is based on an arc-circuit interaction, but to use this approach accurate data and more investigation about the network are necessary (so only described in Appendix A.1).
The second approach is based a black box switching arc models that is programmed in MODELS.
For this model three resistance values of the FCL HTS cable have been used; these values where calculated during the simulations of the three-phase fault current in fault study two (55 Ω; 10,7 Ω

and 5,9 Ω).For these resistances the TRV analysis are done and compared with the standard value that is allowed by the IEC. Except for R = 5,9 Ω, the calculations fulfill the IEC specified values.

Recommendations

Based on the results and conclusions of this research, the following is recommended for future studies:

1. An accurate non-linear characteristic model should be defined for the second generation tape, regarding 150 kV FCL HTS cables.

2. Calculations can be done for longer cable lengths.

3. Single-phase short-circuit fault currents should be studied. In this case it is necessary to have accurate zero-sequence data for the components that will be used in the power network, including the cable.

5. Work-out the current-injection method for this type of cable/network to analyze the TRV behavior.

References

1. **A.Geschiere, D.Willén, E.Piga, P.Barendregt, I.Melnik.**
Optimizing cable layout for long length High Temperature Superconducting Cable. The Netherland, Denmark : Cigré, 2008. B1-307.

2. **Gerard Del-Rosario-Calaf, Andreas Sumper, Xavier Granados, Antoni Sudria-Andreu.**
Grid impact analysis of a HTSC cable by using an enhanced conventional simulator. : IOP Publishing; 9th European Conference on Applied Superconductivity, 2010. Volume 234, Part 3.

3. **John J. Grainger, William D. Stevenson, JR.**
Power System Analysis. : McGraw-Hill International Series, 1994.

4. **Sluis, Lou van der.**
Transients in Power Systems. Sussex : John Wiley, 2002.

5. **Commission, International Electrotechnical.**
IEC 60909-0 Calculation of currents. Geneva : IEC, 2001. IEC 60909-0.

6. **Popov, Marjan.**
Modelling of non-linear elements by ATP-EMTP. Delft, the Netherlands : 2008.

7. **László Prikler, Hans Kr. Høidalen.**
ATPDraw for windows version 1.0. Trondheim : 1998.

8. **Cigré Study committee SC21 HV Insulated Cables.**
High Temperature Superconducting Cable System. Italy : Cigré, June 2003. 229.

9. **Lin Ye, A.M. Campbell.**
Case study of HTS resistive superconducting fault current limiter in electrical distribution systems. China and Cambridge : Elsevier ScienceDirect, 2007.

Appendix

A.1 Arc-circuit current interaction

For this TRV-calculation a known-current (*di/dt*) is injected into the circuit on the fault place. With this value, the *du/dt* of the transient recovery voltage can be calculated. This method will be described for a circuit breaker and how it can be implemented for the FCL HTS cable.

As mentioned in the introduction, the analysis of transients caused by limiting the fault current is compared with a fault current interruption of a circuit breaker. Since the circuit breaker is a sophisticated component, only the aspects of the device that are necessary for this research will be discussed. This is also a reason why basic terms will be mentioned, but not explained in detail.

It is normal that the circuit breaker interrupts a fault-current at current zero. This takes place within microseconds and during this small time frame different processes take place at the same moment. Depending on the configuration of the system the arc-voltage will increase from a constant value (during high current interval) to a peak value (extinction peak) and then drops to zero with a very steep *du/dt*. Immediately after the current interruption the TRV takes place. The TRV that is caused by the transfer of energy in the power system can be expressed by *du/dt* or *kV/μs*. The total amount of time that the TRV is present in the circuit is in the order of milliseconds. This is quite short, when considering that the frequency of the system is 50 Hz. Still the rate of rise of the recovery voltage is essential, because the components in the network should be able to withstand the overvoltage.

When considering a circuit breaker it is possible that after a current interruption a scarce so-called *post-arc current* occurs. This is caused by the physical processes that have taken place in the arc channel, during current interruption. The reason for mentioning the post-arc current is because it is caused by the steep rate of rise of recovery voltage, in combination with other processes inside the arcing chamber of the circuit breaker.

During a current interruption process there is a strong interaction concerning the physical process between the circuit breaker contacts and the network connected with the terminals of the breaker. The driving voltage and the total series inductances formed by all the components in the system will determine the current, during the interruption process. The *di/dt* can be derived from the short-circuit current:

$$\boldsymbol{i(t) = Isin(\omega t)} \qquad \text{[A.1.1]}$$

$$\boldsymbol{\frac{di}{dt} = \omega Icos(\omega t) = 2\pi f I_{rms}\sqrt{2}cos(\omega t)} \qquad \text{[A.1.2]}$$

For t = 0: $\boldsymbol{di/dt = 2\pi f I_{rms}\sqrt{2} = 0,444 I_{rms}}$ for 50 Hz. And if I_{rms} is entered in kA, the *di/dt* is in $A/\mu s$.

In ATP a current source injects a current of 1kA on the fault place. This 1kA is associated with the $0.444I_{rms}$, which is modeled with MODELS. This is the initial condition of this calculation method, as depicted in Figure 44. The steepness of the current is 0,444 A/µs.

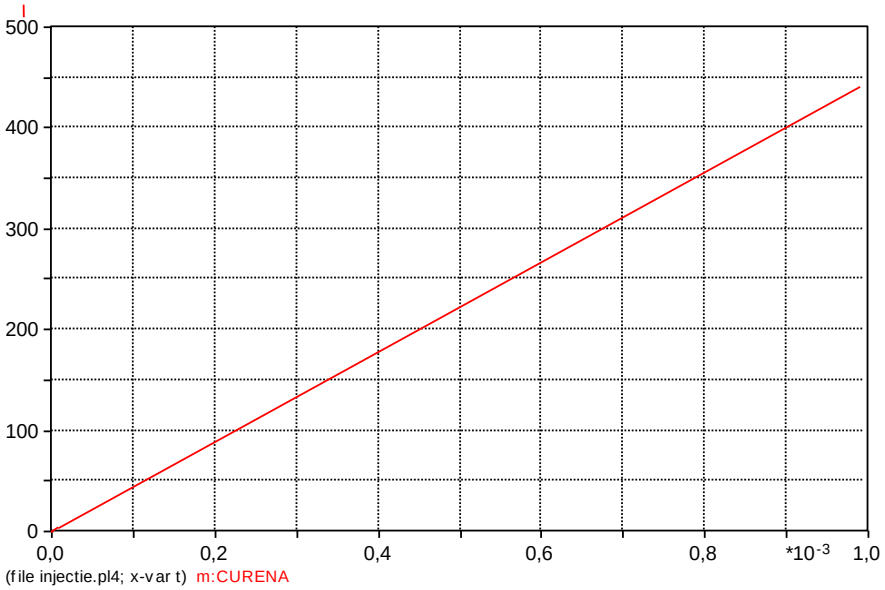

Figure 44: Injected current wave at fault place (x-axis: time in s and y-axis: current in A)

In Figure 45 the network circuit, for calculating the TRV through current injection method, is depicted.

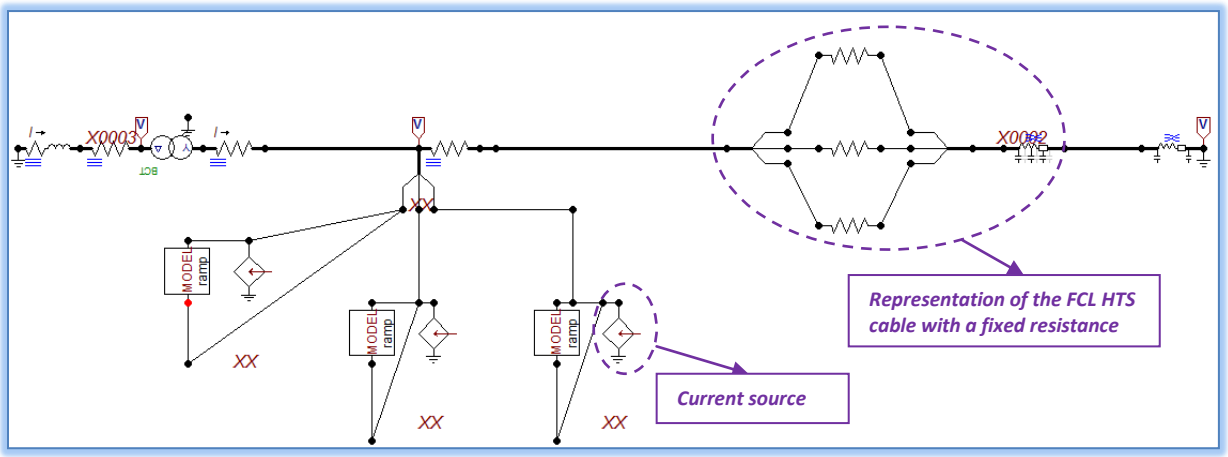

Figure 45: Injected current source at fault place

This network is basically the same as used for the short-circuit analysis (fault study two), but now the voltage sources are eliminated and replaced by current sources. As mentioned before a known-current is injected into the circuit, for all three-phases. This is done by using a single-phase current source, as an input for MODEL; in MODELS the slope 0,444 A/µs is determined and inserted in the

circuit. In Table 12 the data-, input- and output parameters for MODELS are given. The data values are user-defined parameters, the input values come from the power circuit and the output values are inserted in the network.

DATA		VALUE	SYMBOL
amplitude		444	
width		0,001	
INPUT		voltage (V)	
OUTPUT		current (A)	
ATP SIMULATION SETTINGS: time domain			
DATA PARAMETER	**UNIT**	**VALUE**	
delta_T	s	1.10^{-6}	
Tmax	s	0,001	

Table 12: Data-parameters for MODELS_current injection method

The resistance of the FCL HTS cable is a fixed value in this circuit and it is independent from the current because it is determined from fault study two. For this analysis, for all three-phases, the resistances that are determined from the short-circuit studies are inserted to analyze the TRV response. In Figure 46 the TRV response with R = 55 Ω is inserted. Finally the du/dt of the TRV can be calculated for the simulation of Figure 46 (with a fault current of 1 kA).

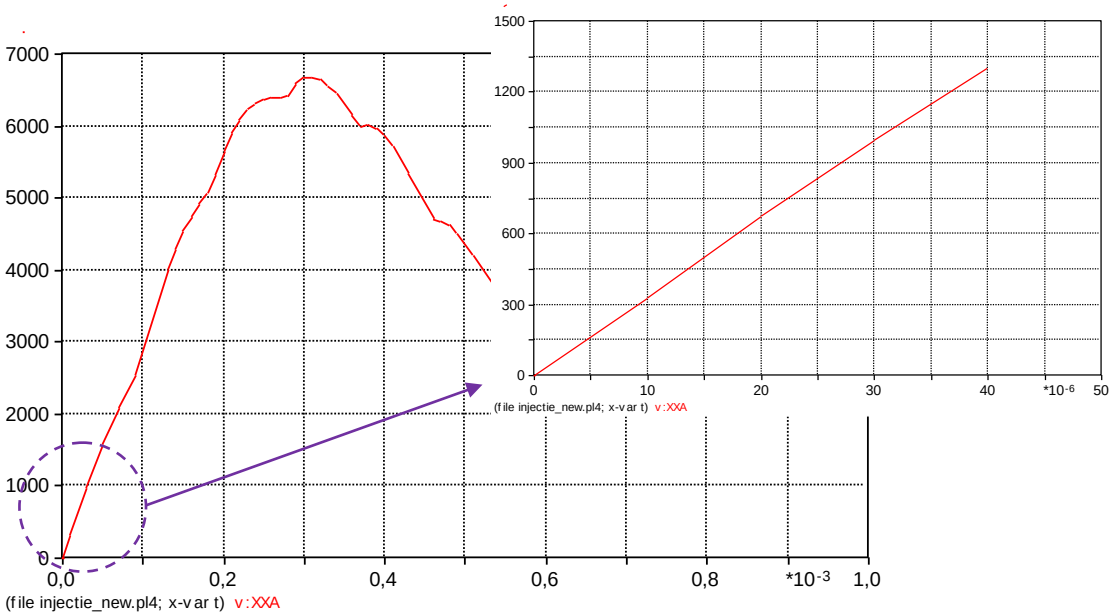

Figure 46: TRV-response for fault current of 1kA, with R = 55 Ω (x-axis: time in s and y-axis: voltage in V)

The following values for the time in µs and voltage in V are read from the plot. With the equation in the last row the *du/dt* of the TRV, for 1 kA, is calculated in Table 13.

R = 55 Ω			
Time µs		**Voltage V**	
t_1	30	u_1	997,55
t_2	40	u_2	1300,2
Δt	10	Δu	302,65
$\frac{du}{dt} = \frac{u2-u1}{t2-t1} = 30{,}27\frac{V}{us} = 0{,}03\frac{kV}{us}$			
***du/dt* for 40 kA is: 0,03 ∗ 40 = 1,2 kV/µs**			

Table 13: du/dt calculation for 1 kA (with R = 55 Ω)

The TRV response of the other resistance values are determined in the same way and the results are presented in Table 14 and Table 15.

R = 10,7 Ω			
Time µs		**Voltage V**	
t_1	30	u_1	501,13
t_2	40	u_2	663,71
Δt	10	Δu	162,58
$\frac{du}{dt} = \frac{u2-u1}{t2-t1} = 16{,}3 = 0{,}02\frac{kV}{us}$			
***du/dt* for 40 kA is: 0,02 ∗ 40 = 0,8 kV/µs**			

Table 14: du/dt calculation for 1 kA (with R = 10,7 Ω)

R = 5,92 Ω			
Time µs		**Voltage V**	
t_1	30	u_1	444,59
t_2	40	u_2	589,87
Δt	10	Δu	145,28
$\frac{du}{dt} = \frac{u2-u1}{t2-t1} = 14{,}5 = 0{,}01\frac{kV}{us}$			
***du/dt* for 40 kA is: 0,01 ∗ 40 = 0,4 kV/µs**			

Table 15: du/dt calculation for 1 kA (with R = 5,92 Ω)

These values are lower than the values determined in paragraph 9.2. The conclusion is that, even though this method is applied easily to calculate transients, in this case it does not completely satisfy the expectations. It does not mean that the method is not correct, but accurate data and more investigation about the network are necessary.

A.2 Graphical determination of factor κ

The value for κ can also be obtained from the following figures. This parameter depends on the R/X or X/R ratio. These graphs are taken from IEC 60909, page 101.

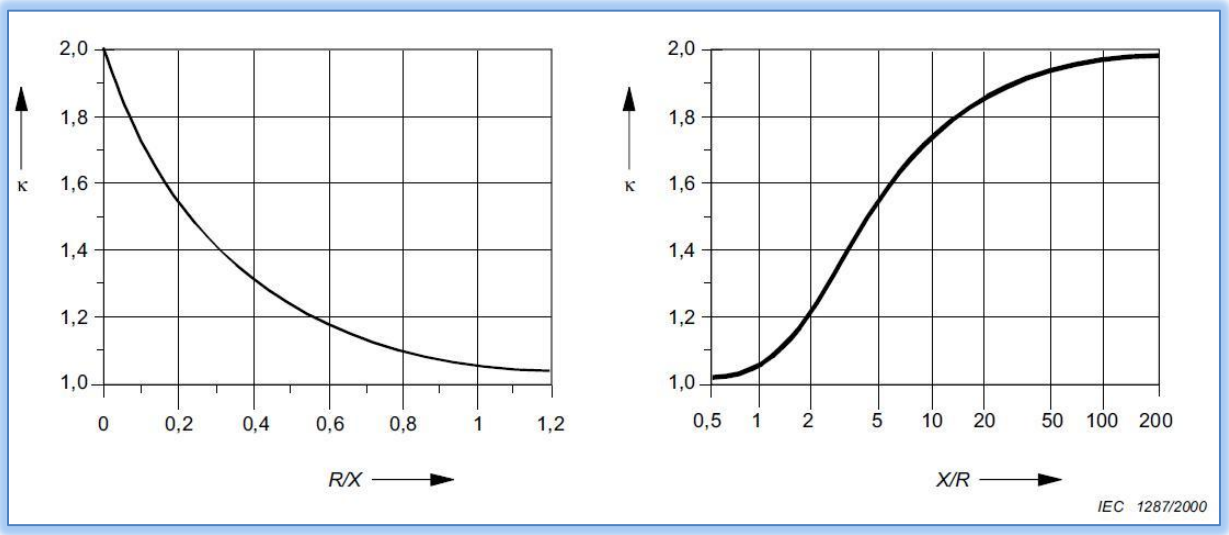

Figure 47:Factor κ as a function of ratio R/X or X/R

A.3 Extra simulation results of fault studies

For readers who are interested in all the fault study simulation results, these will be depicted in this part of the appendix (**for all three phases**).

A.3.1 Three-phase fault simulated between the 150 kV infinite grid and the 150 kV FCL HTS cable

1. Generator terminal voltage:

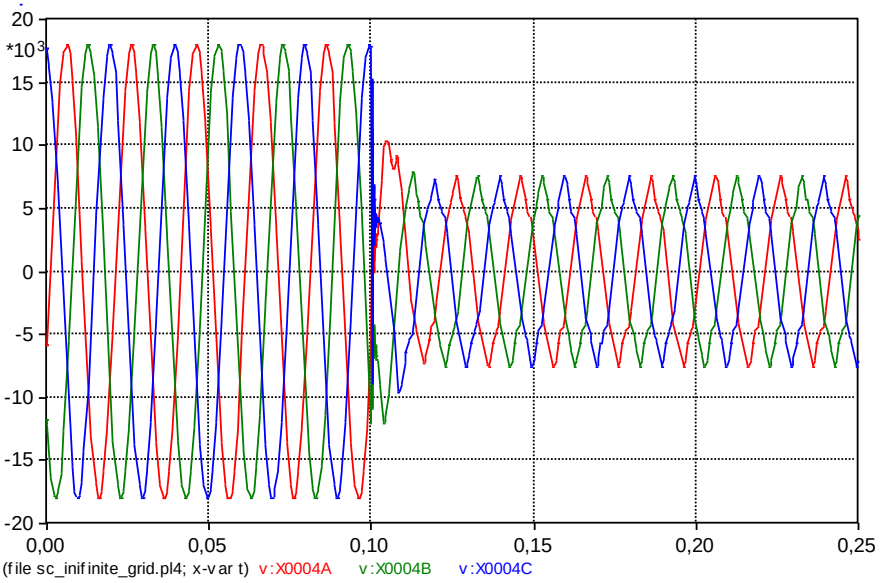

Figure 48: Voltage across the generator terminal, during a fault between cable and infinite grid (y-axis: voltage in kV; x-axis: t in s)

2. Fault current provided by the generator:

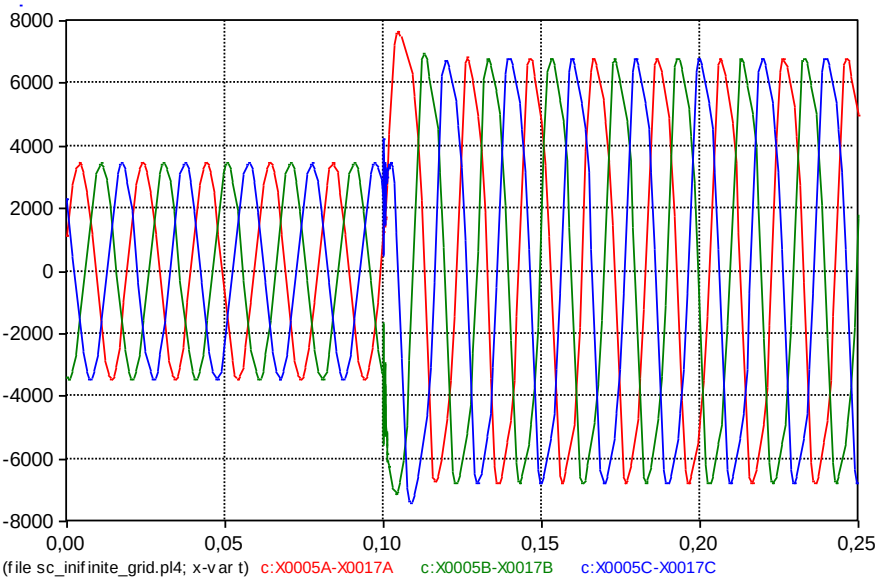

Figure 49: Three-phase fault to earth between cable and infinite grid, provided by the generator (x-axis: time in s and y-axis: current in A)

3. Fault current provided by the infinite grid:

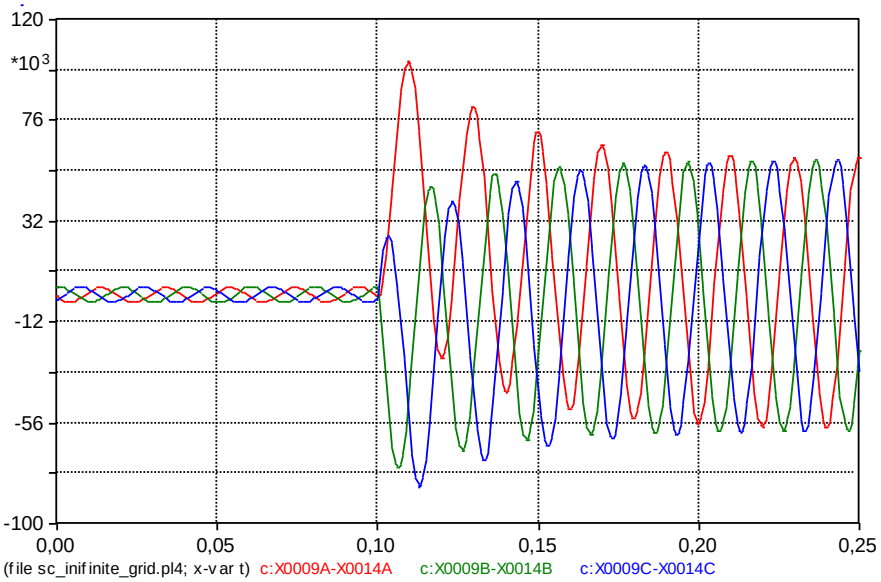

Figure 50: Three-phase fault to earth between cable and infinite grid provided by the infinite grid (x-axis: time in s and y-axis: current in A)

4. Total three-phase fault current to earth:

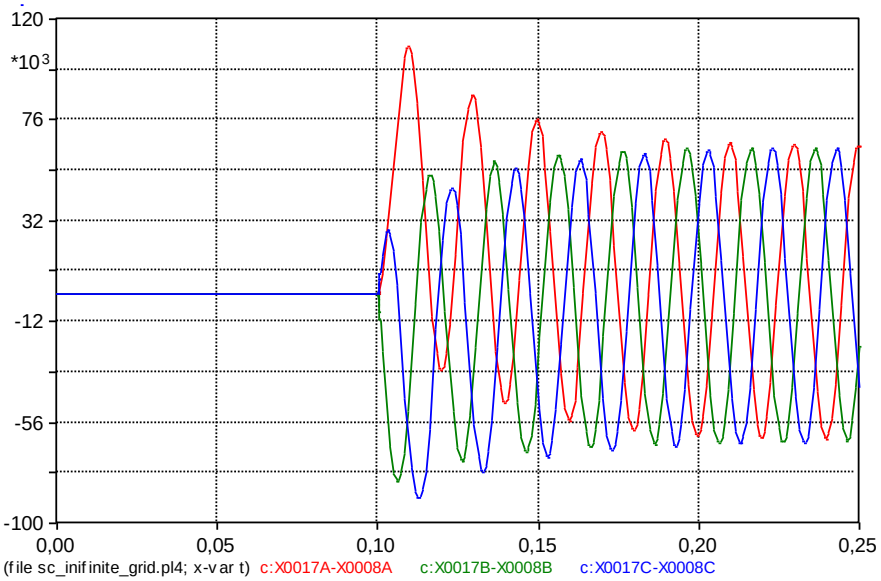

Figure 51: Total three-phase fault to earth between cable and infinite grid (x-axis: time in s and y-axis: current in A)

A.3.2 Three-phase fault simulated between the 23/150 kV transformer and the 150 kV FCL HTS cable

1. Generator terminal voltage:

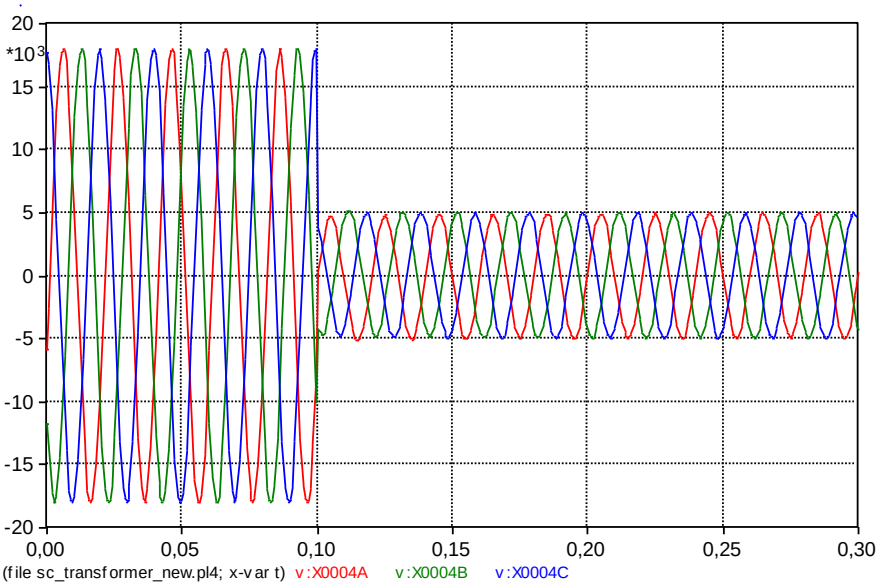

Figure 52: Voltage across the generator terminal, during a fault between cable and transformer (y-axis: voltage in kV; x-axis: t in s)

2. Fault current provided by the generator:

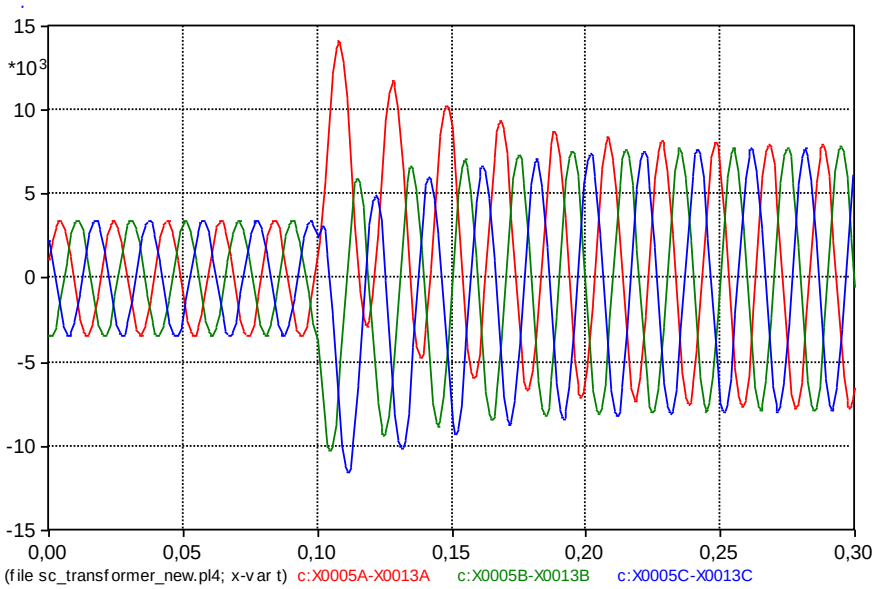

Figure 53: Three-phase fault to earth between cable and transformer, provided by the generator (x-axis: time in s and y-axis: current in A)

3. Fault current provided by the infinite grid:

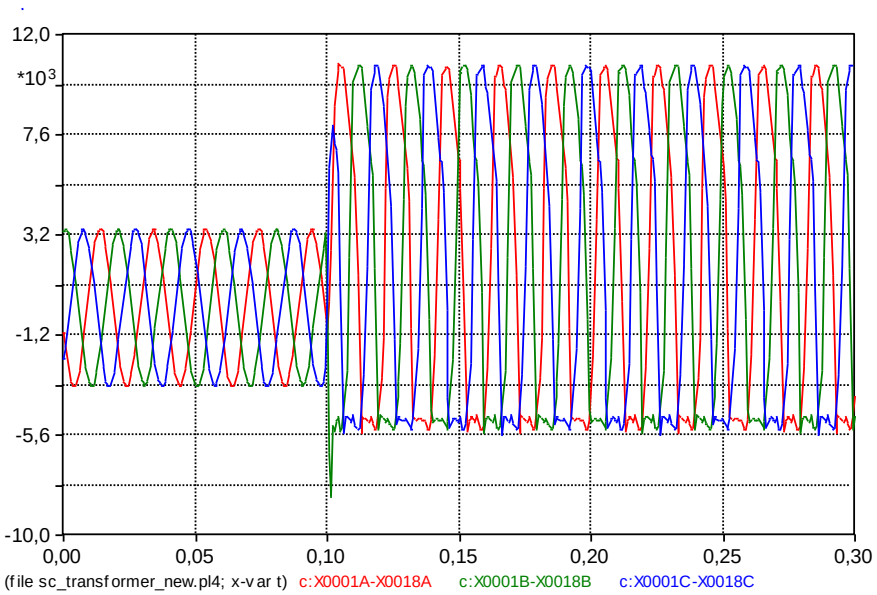

Figure 54: Three-phase fault to earth between cable and transformer, provided by the infinite grid (x-axis: time in s and y-axis: current in A)

4. Total three-phase fault current to earth:

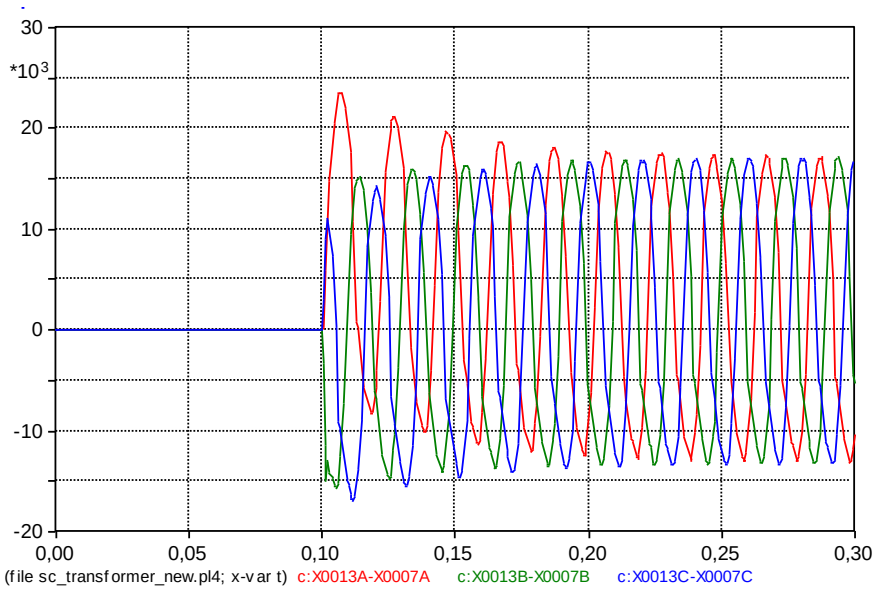

Figure 55: Total three-phase fault to earth between cable and transformer (x-axis: time in s and y-axis: current in A)